Journal of Medicinal Chemistry

Article

Triazole Ureas act as Diacylglycerol Lipase Inhibitors and Prevent Fasting-induced Refeeding

Hui Deng, Sander Kooijman, Adrianus M.C.H. van den Nieuwendijk, Daisuke Ogasawara, Tom van der Wel, Floris van Dalen, Marc P. Baggelaar, Freek J. Janssen, Richard J.B.H.N van den Berg, Hans den Dulk, Benjamin F. Cravatt, Herman S. Overkleeft, Patrick C.N. Rensen, and Mario van der Stelt

J. Med. Chem., **Just Accepted Manuscript** • DOI: 10.1021/acs.jmedchem.6b01482 • Publication Date (Web): 07 Dec 2016

Just Accepted

ACS Publications

Journal of Medicinal Chemistry is published by the American Chemical Society. 1155 Sixteenth Street N.W., Washington, DC 20036

Triazole Ureas act as Diacylglycerol Lipase Inhibitors and Prevent Fasting-induced Refeeding

Hui Deng [†], Sander Kooijman [§], Adrianus M.C.H. van den Nieuwendijk [‡], Daisuke Ogasawara [∥], Tom van der Wel [†], Floris van Dalen [†], Marc P. Baggelaar [†], Freek J. Janssen [†], Richard J.B.H.N. van den Berg [‡], Hans den Dulk [†], Benjamin F. Cravatt [∥], Herman S. Overkleeft [‡], Patrick C.N. Rensen [§] & Mario van der Stelt [†,]*

[†] Department of Molecular Physiology, Leiden Institute of Chemistry, Leiden University, Leiden, The Netherlands.

[‡] Department of Bioorganic Synthesis, Leiden Institute of Chemistry, Leiden University, Leiden, The Netherlands.

[§] Department of Medicine, Division of Endocrinology and Einthoven Laboratory for Experimental Vascular Medicine, Leiden University Medical Center, Leiden, The Netherlands.

[∥] Department of Chemical Physiology, The Scripps Research Institute, La Jolla, California, United States of America.

ABSTRACT

Triazole ureas constitute a versatile class of irreversible inhibitors that target serine hydrolases both in cells and animal models. We have previously reported that triazole ureas can act as selective and CNS-active inhibitors for diacylglycerol lipases (DAGLs), enzymes responsible for the biosynthesis of 2-arachidonoylglycerol (2-AG) that activates cannabinoid CB_1 receptor. Here, we report the enantio- and diastereoselective synthesis and structure-activity relationship studies. We found 2,4-substituted triazole ureas with a biphenylmethanol group provided the most optimal scaffold. Introduction of a chiral ether substituent on the 5-position of the piperidine ring provided ultrapotent inhibitor **38** (DH376) with picomolar activity. Compound **38** temporarily reduces fasting-induced refeeding of mice, thereby emulating the effect of cannabinoid CB_1-receptor inverse agonists. This was mirrored by **39** (DO34), but also by the negative control compound **40** (DO53) (that does not inhibit DAGL), which indicates the triazole ureas may affect the energy balance in mice through multiple molecular targets.

INTRODUCTION

Compound libraries that contain a 1,2,3-triazole urea scaffold have previously been applied to the discovery of potent inhibitors of diverse serine hydrolases, such as diacylglycerol lipase-β (DAGLβ), α,β-hydrolase domain (ABHD) 6/11, DDHD2, APEH and PAFAH2.[1-5] 1,2,3-Triazole ureas constitute a versatile chemotype for the covalent, irreversible and selective inhibition of serine hydrolases. They contain an electrophilic carbonyl group with tunable reactivity as well as a scaffold to introduce functional groups conferring enzyme potency and/or specificity. 1,2,3-Triazole ureas irreversibly inhibit serine hydrolases via carbamoylation of the active-site serine nucleophile. Some reported triazole urea inhibitors were proven to be potent and selective for specific serine hydrolases both in cells and mouse models, and are effective chemical probes to study the biological function of serine hydrolases in diverse biological systems.[1, 2] For example, **1** (KT109)[4], a selective and *in vivo*-active DAGLβ inhibitor reduces 2-arachidonoylglycerol (2-AG), arachidonic acid and eicosanoids levels in peritoneal macrophages of lipopolysaccharide (LPS)-treated mice and significantly decreases the pro-inflammatory cytokine, tumour necrosis factor α (TNFα) in LPS-treated mice.[4]

Two isoforms of DAGL exist, and that are expressed in a tissue-dependent manner. Both isoforms, termed DAGLα and DAGLβ employ a Ser-His-Asp catalytic triad characteristic for serine hydrolases to hydrolyse an ester bond of diacylglycerol (DAG) in a *sn*-1 specific manner. DAGLα and DAGLβ share extensive homology, but differ in size: DAGLα is about 120 kDa and DAGLβ is around 70 kDa.[6, 7] DAGLα is the principal regulator of 2-AG formation in the nervous system, where it controls the activity of this endocannabinoid, which activates the cannabinoid CB_1 receptor, as a retrograde

messenger at neuronal synapses. DAGLβ in turn is the dominant enzyme for 2-AG production in the periphery during inflammation.[8, 9]

To study the function of DAGLs in a temporal and dynamic manner, *in vivo*-active inhibitors of these enzymes would be of great value. Particularly, a CNS-active chemical probe is required for DAGLα (mainly expressed in the brain) that can be used to acutely perturb 2-AG production in the central nervous system. The known DAGL inhibitors can be classified into six different chemotypes: α-ketoheterocycles, glycine sulfonamides (both reversible, competitive DAGL inhibitor classes), bis-oximino-carbamates, β-lactones, fluorophosphonates and 1,2,3-triazole ureas (the latter four being mechanism-based and irreversible).[4, 10-14] These inhibitors have been used to study the function of 2-AG in cellular models and brain slice preparations, but they lack selectivity over serine hydrolases, potency and/or chemical properties required for central activity. Of note, with the exception of the α-ketoheterocycles, all DAGL inhibitors reported to date also inhibit ABHD6. Since the latter enzyme hydrolyses the DAGL product 2-AG, relating the physiological effect of such dual inhibitors to modulating 2-AG levels through DAGL inactivation is complicated.

We selected compound **1** as a suitable starting point for the rational design of new, potent and selective inhibitors for DAGLα, because it inhibits DAGLα with an IC_{50} of 2.3 μM in a competitive activity-based protein profiling (ABPP) assay.[4] In a first round of optimization, we converted compound **1** into **38** (DH376), a highly potent, *in vivo* active compound that inhibits DAGLα in a time- and dose dependent manner in mouse brain.[15] Using compound **38**, as well as the structurally distinct compound **39** (DO34)[15] (see Supporting Information, Figure S6), we performed functional studies on DAGLα in

nervous system.[15] We found that DAGLs coordinate crosstalk between several brain lipid signalling networks and modulate neuro(immuno)logical functions in central nervous system.

Here, we provide a full account of the discovery, development and *in vivo* efficacy data of compound **38** as an inhibitor of DAGLα.[15] We systematically investigated the influence of regioselectivity of the 1,4- and 2,4-triazole moiety, the nature of the substituents on the triazole core, the chirality of the benzylpiperidine and the substituent pattern of the piperidine ring on DAGLα and ABHD6 activity. To this end, we developed an enantioselective synthesis route to obtain both enantiomers of the benzylpiperidines and their derivatives. Finally, we determined the selectivity profiles of the 1,2,3-triazole ureas in mouse brain membrane proteome and assessed whether compound **38** is able to inhibit fasting-induced refeeding in mice, a typical cannabinoid CB_1 receptor mediated response.

RESULTS AND DISCUSSION

Discovery of 2,4-substituted 1,2,3-triazole urea as new chemotype of DAGLα inhibitor.

In our search for CNS-active DAGLα inhibitors, we employed a rational design drug discovery approach in which compound **1** and a closely related analogue, **2** (ML226)[1], served as starting points (structures are shown in Figure 1). Compound **1** is a peripherally restricted DAGLβ inhibitor with 60-fold selectivity over DAGLα. Compound **2** in turn, is a potent, cellular and *in vivo* active ABHD11 inhibitor with excellent physicochemical properties.[1, 4] First, we tested the activity of compounds **1** and **2** on HEK293T membranes overexpressing human DAGLα and mouse DAGLβ in a colorimetric assay using *para*-

nitrophenylbutyrate (PNP) as a surrogate substrate (Figure 1b, c; Table S.1 in supporting information).[10, 11] We found that compound **1** inhibited mouse DAGLβ with a pIC_{50} of 7.1 ±0.2, which is consistent with previously reported in a gel-based ABPP assay using HT-01 as a chemical probe (pIC_{50} = 7.4)[4]. However, compound **1** (pIC_{50} 8.9±0.1) was much more potent on human DAGLα in our assay, than previously reported in a gel-based ABPP assay using HT-01 as a chemical probe (pIC_{50} = 5.6)[4]. The difference might be due to the weak labeling efficiency of HT-01 for DAGLα. In contrast, compound **2** demonstrated weak DAGLα activity with a pIC_{50} 7.2±0.1 and poor DAGLβ activity in the PNP-assay. At first sight this is in line with the previously reported preference of DAGLβ for 1,4-regioisomers of the triazole ureas over the corresponding 2,4-regioisomers.[16] Compound **2** lacks, however, the 2-benzyl substituent on the piperidine moiety for an appropriate comparison between the two inhibitors. Therefore, we synthesized compounds **3**-**6** as hybrid structures harbouring elements of both compounds **1** and **2**. To this end, the triazole building blocks and the final compounds were synthesized as previously reported (see supporting information). Interestingly, compound **4**, a 2-benzylpiperidine urea of a 2,4-triazole with a 1,1-diphenylmethanol substituent at the 4-position (as in compound **2**), showed the highest DAGLα and DAGLβ inhibitory activity with pIC_{50} of 8.6±0.1 and 7.9±0.1, respectively. Its 1,4-regioisomer (compound **3**) is 10-fold less potent. This indicates that 2,4-triazole is the preferred regioisomer for DAGLα and DAGLβ inhibition (Figure 1d, e; Table S.1 in supporting information). Hybrid compounds (**5** and **6**) with an ethyl substituent at the 2-position of the piperidine ring appeared less potent than compound **1**, which suggests that the benzyl substituent is required to address an additional lipophilic pocket near the active site in the enzymes

(Figure 1d, e). We next employed competitive ABPP assays to confirm the inhibitory activities of compounds **1-6** against recombinant human DAGLα and human DAGLβ. A previously reported DAGL-tailored activity-based probe-DH379 was used for these studies. [15] The results of gel-based ABPP assay were in line with the above PNP-assay that compound **1** potently inhibited DAGLα and DAGLβ labeling by DH379, and compound **4** showed the highest potency against human DAGLα and DAGLβ among the hybrid compounds (Figure 1 f and g; Figure S.1 in supporting information).

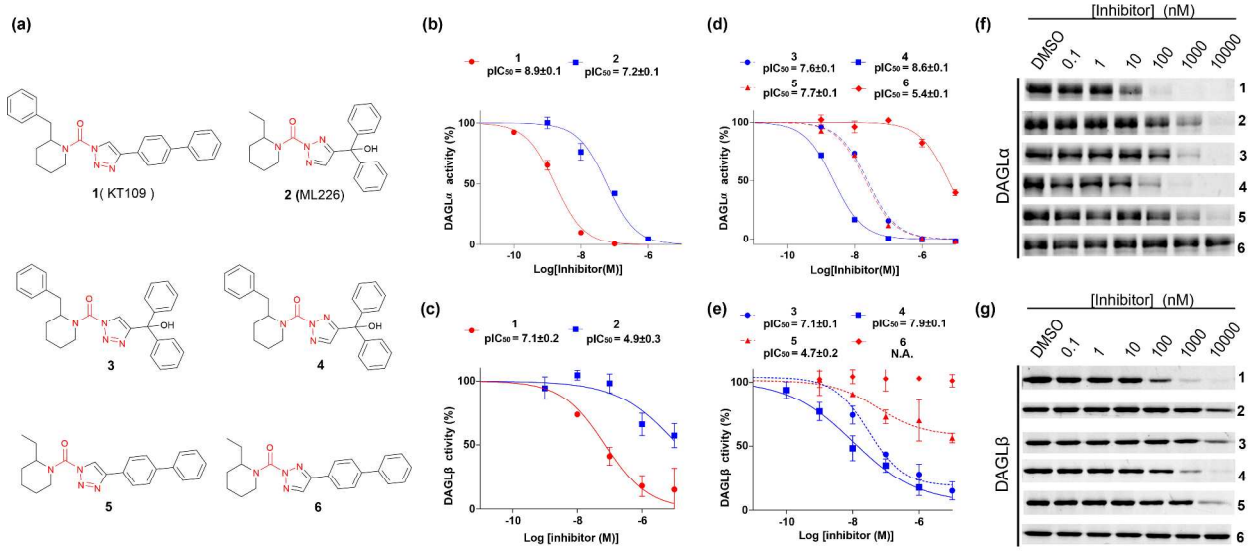

Figure 1. (a) The structures of 1,2,3-triazole ureas **1-6**. (b, d) Concentration-dependent inhibition of recombinant human DAGLα by compounds **1-6** as measured with a colorimetric assay based on the hydrolysis of PNP butyrate in DAGL-transfected HEK293T cells. (c, e) Concentration-dependent inhibition of recombinant mouse DAGLβ by compounds **1-6** as measured with PNP butyrate substrate assay. Data represent average values ± SEM; n = 4 per group. (f, g)

Representative fluorescent gel-based competitive ABPP with compound **1-6** against recombinant human DAGLα and DAGLβ by tailored activity-based probe DH379 (1 μM, 30 min).

We next investigated the contribution of the phenyl groups of the 1,1-diphenylmethanol substituent in compound **4** to DAGLα inhibition (Table 1). To this end, we replaced the phenyl rings by cyclohexyls (**7**, **8**); removed one (**9**) or both (**10**) phenyl groups; replaced them by a pyridyl (**11**) or introduced fluorine atoms (**12**). The biochemical assay revealed that *para*-fluoro substituted inhibitor (**12**) was the most potent agent in this series against hDAGLα with a pIC_{50} of 9.0, which suggested that its increased lipophilicity and/or electron withdrawing effect is beneficial. The ~100-fold drop in potency of the more polar pyridyl-containing compound (**11**), suggested that lipophilicity is more important than electron withdrawing properties. Indeed, the lipophilic interactions of the phenyl groups are essential features of the DAGLα inhibitor, because their removal led to a 160-2000 fold decrease in potency (**8**-**10**), whereas retaining two bulky cyclohexyl groups (**7**) resulted in only a 40-fold drop in potency. A role for pi-sigma/cation interactions can, however, also not be excluded. A 10-fold decrease in potency was observed when the tertiary alcohol group was methylated, as in compound (**13**), suggesting that a hydrogen bond donor is important (or alternatively, the grafted methyl group has a steric clash with the enzyme). To reduce the lipophilicity we substituted the 2-benzyl substituent of the piperidine ring for a phenoxymethyl- (**14**, **15**) or (4-fluoro)phenoxymethyl group (**16**, **17**) and introduced polar methoxy substituents on the phenyl ring (**18**, **19**). The substitutions were tolerated (Table 1), but led to a five-fold reduced activity.

Table 1. Structure-activity relationship of triazole ureas with N2-isomers as leaving groups

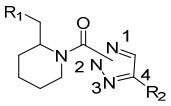

Entry	R_1	Regio-isomer	R_2	pIC_{50}±SEM (DAGLα)	pIC_{50}±SEM (ABHD6)
3		1,4-	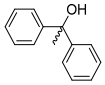	7.6±0.1	7.4±0.1
4		2,4-	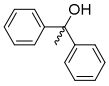	8.6±0.1	7.7±0.1
7		2,4-	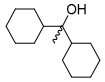	7.0±0.1	5.1±0.2
8		2,4-		5.8±0.1	5.5±0.1
9		2,4-		6.4±0.1	5.5±0.1
10		2,4-		5.3±0.2	<5
11		2,4-	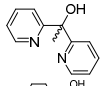	6.8±0.1	5.5±0.2
12		2,4-	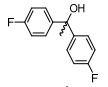	9.0±0.1	7.6±0.1
13		2,4-	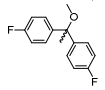	7.9±0.2	<5
14		2,4-		8.1±0.1	6.8±0.1
15		2,4-	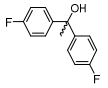	8.3±0.1	6.7±0.1
16		2,4-	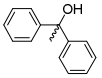	8.2±0.1	6.6±0.1
17		2,4-	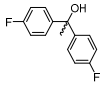	8.3±0.1	6.7±0.1
18		2,4-	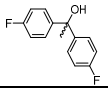	8.5±0.5	6.8±0.2

19		2,4-	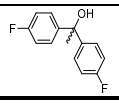	8.3±0.1	6.6±0.1

29a is the most active DAGL inhibitor.

Previously, the eutomer of compound **1** was found to be 100-fold more potent than the distomer against DAGLβ.[16] The absolute configuration of the enantiomers was, however, not assigned. To determine whether **29a** or **29b** is the most active enantiomer, we developed a novel enantioselective synthesis route (Scheme 1 and Supporting Information). Our synthesis of the separate enantiomers of compound **1** began with the preparation of chiral amine **23a** in four steps from commercially available Boc-protected L-phenyl alanine **20a**.[17] We reacted amine **23a** with 3-pentene nitrile **24** to give secondary amine **25a** via a one-pot DIBAL-H reduction-transimination-$NaBH_4$ reduction sequence.[18] Subsequent Boc-protection of the amine, ring-closing metathesis, hydrogenation and Boc-deprotection led to the construction of the key chiral 2-benzylpiperidine building block **28a** in a 44% overall yield. Direct coupling of the chiral piperidine with 4-([1,1'-biphenyl]-4-yl)-1*H*-1,2,3-triazole using triphosgene, provided final compound **29a** in >95% e.e. as determined by chiral HPLC. The synthesis of the other enantiomer **29b** proceeded in a similar fashion using chiral amine **23b** (see Supporting Information, Scheme S.3).

To correlate the activity of the compounds with their stereochemistry, we tested both compounds and a 1:1 mixture in the colorimetric surrogate PNP-substrate assay using HEK293T membranes expressing recombinant human DAGLα. Compound **29a** proved to be the eutomer with a pIC_{50} of 9.1±0.1, while compound **29b** showed ~100-fold less

activity (pIC_{50} of 7.4±0.1) (Figure 2a) in the PNP-assay. The 1:1 racemic mixture demonstrated a pIC_{50} of 8.2±0.1. We also employed a real-time, fluorescence-based assay to test the activity of the inhibitors on DAGLα-mediated hydrolysis of its natural substrate 1-stearoyl-2-arachidonoly-*sn*-glycerol.[19] Again, compound **29a** was the most active DAGLα inhibitor with a pIC_{50} of 7.6±0.1 (Figure 2b). Since ABHD6 was previously reported as an off-target of compound **1**, we also tested the activities of both enantiomers (**29a** and **29b**) against human ABHD6.[11, 20] Compound **29a** (pIC_{50} 8.6±0.1) was ~100-fold more potent than **29b** (pIC_{50} 6.2±0.1) (Figure 2c), which indicates that the inhibitory activity for both DAGLα and ABHD6 resides in the (*R*)-enantiomer. To assess the activity and selectivity of compounds **29a** and **29b** on endogenously expressed DAGLα in mouse brain membrane proteome, we used the previously reported ABPP method with MB064, a tailored activity-based probe.[10] Consistent with the biochemical assays, we found that compounds **29a** and **29b** blocked DAGLα labeling by MB064 with pIC_{50} of 8.1±0.1 and 6.2±0.1, respectively (Figure 2d and Figure S.2).

Scheme 1. Enantioselective synthesis of **29a**

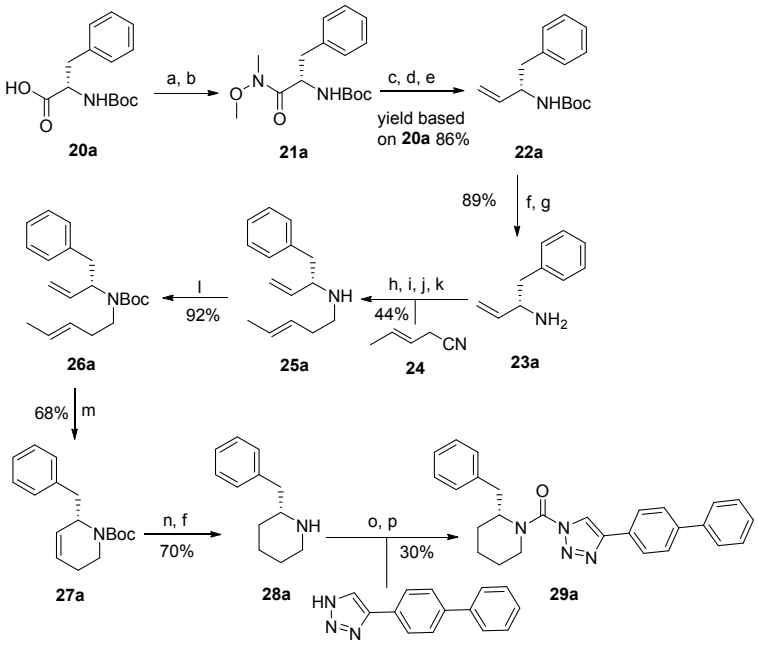

Reagents and conditions: (a) Me(OMe)NH·HCl; (b) EDCI, NMM; (c) $LiAlH_4$; (d) H_3O^+; (e) $(Ph)_3P{=}CH_2$; (f) MeOH, HCl; (g) NaOH; (h) **24**, diethyl ether, DIBAL-H, -80 ^oC to 0 ^oC; (i) MeOH, -90 ^oC; (j) corresponding amine **23a** (3 equiv), r.t., 20h; (k) $NaBH_4$, 0 ^oC to r.t., 5h; (l) Boc_2O, Et_3N, THF, 50 ^oC, 20h; (m) Grubbs I cat. 4 mol%, DCM, reflux, 48h; (n) H_2, Pd/C, MeOH; (o) DIPEA, triphosgene, THF, 0 ^oC; (p) DIPEA, DMAP, triazole , THF, 60 ^oC.

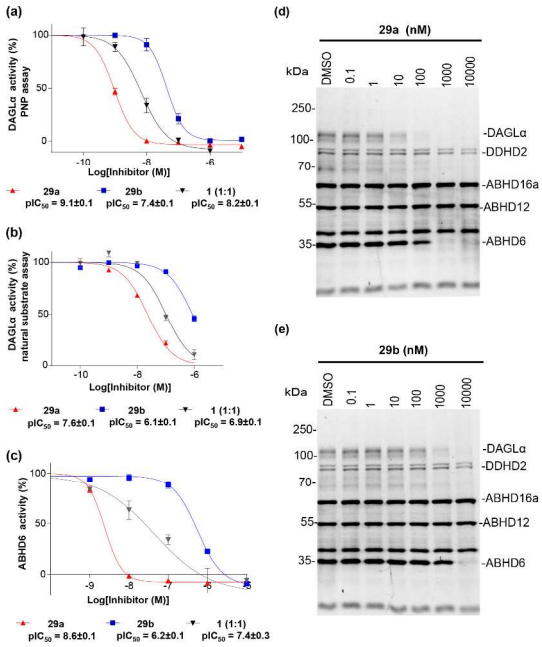

Figure 2. Characterization of both enantiomers of compound **1** as DAGLα inhibitors: (a) Concentration-dependent inhibition of recombinant hDAGLα by **29a**, **29b** and racemic compound **1** (1:1) as measured with a colorimetric assay based on the hydrolysis of PNP butyrate. (b) Concentration-dependent inhibition of recombinant hDAGLα by **29a**, **29b** and racemic compound **1** (1:1) as measured with a SAG substrate assay in DAGLα-transfected HEK293T cells. (c) Concentration-dependent inhibition of hABHD6 by **29a**, **29b** and racemic compound **1** (1:1) as measured with a 2-AG substrate assay. Data represent average values ± SEM; n = 4 per group. (d, e) Representative fluorescent gel-based competitive ABPP with **29a** and **29b** in mouse brain proteome by tailored activity-based probe MB064 (0.25 μM, 30 min).

Discovery of highly potent DAGL inhibitors.

Having discovered that the (*R*)-enantiomer is the most active compound in the 1,4-triazole series, we transferred this knowledge to the 2,4-triazole series. To this end we coupled the chiral amine building block **23a** to the triazole scaffold to provide compound **(*R*)-12**. We found that **(*R*)-12** had a pIC_{50} of 9.1±0.1, which was slightly higher than the racemic mixture (Figure 3a). To improve solubility and to mimic the natural substrate diacylglycerol, we designed several new analogues with a chiral hydroxyl group at the C-5 position (Scheme 2 and S.4; **30**-**33**). The chiral, diastereomers were synthesized according to Scheme 2. In short, the cyanohydrin **40** was enzymatically produced by the almond (*R*)-hydroxynitrile lyase using crotonic aldehyde **39** as a substrate.[21] After silyl protection of the alcohol, we generated key intermediate **44** by the same strategy as described for the synthesis of **29a**. After *N*-Boc deprotection, and optional hydrogenation, compounds **45** and **48**, were coupled to the 1,2,3-triazole building block, yielding *O*-silyl protected intermediates **46** and **49**. Deprotection gave (final) compounds **30** and **31**. Further alkylation of intermediate **50**, *N*-Boc deprotection and coupling with 1,2,3-triazole building block afforded compounds **34** and **35**. Compounds **32**, **33**, **36** and **37** were synthesized in the same fashion as described for the corresponding diastereoisomers (Scheme S.4).

We tested compounds **30**-**38** in the PNP-assay and found that the free alcohol derivatives **30**-**33** are less potent than compound **12** (Table 1 and 2). Capping the secondary hydroxyl group with an alkyl moiety yielded (ultra) potent inhibitors. For example, compounds **34** and **35** demonstrated picomolar activity with pIC_{50} values of 9.1±0.1 and 9.2±0.1, respectively (Table 2). Comparison of the diastereoisomers (**34** vs **36**; **35** vs **37**) revealed that the back isomer at C-5 is the active diastereomer (**34**, **35**)

(with ~10-fold higher potency). To visualize target engagement, we surmised that we could introduce a propargyl at C-5, which serves as a ligation handle to introduce reporter groups by copper-catalyzed azide-alkyne cycloaddition (or "click"-chemistry). This yielded inhibitor **38** with a pIC_{50} = 8.9±0.1.

Scheme 2. Enantioselective synthesis of 1,2,3 triazole ureas **30**, **31**, **34** and **35.**

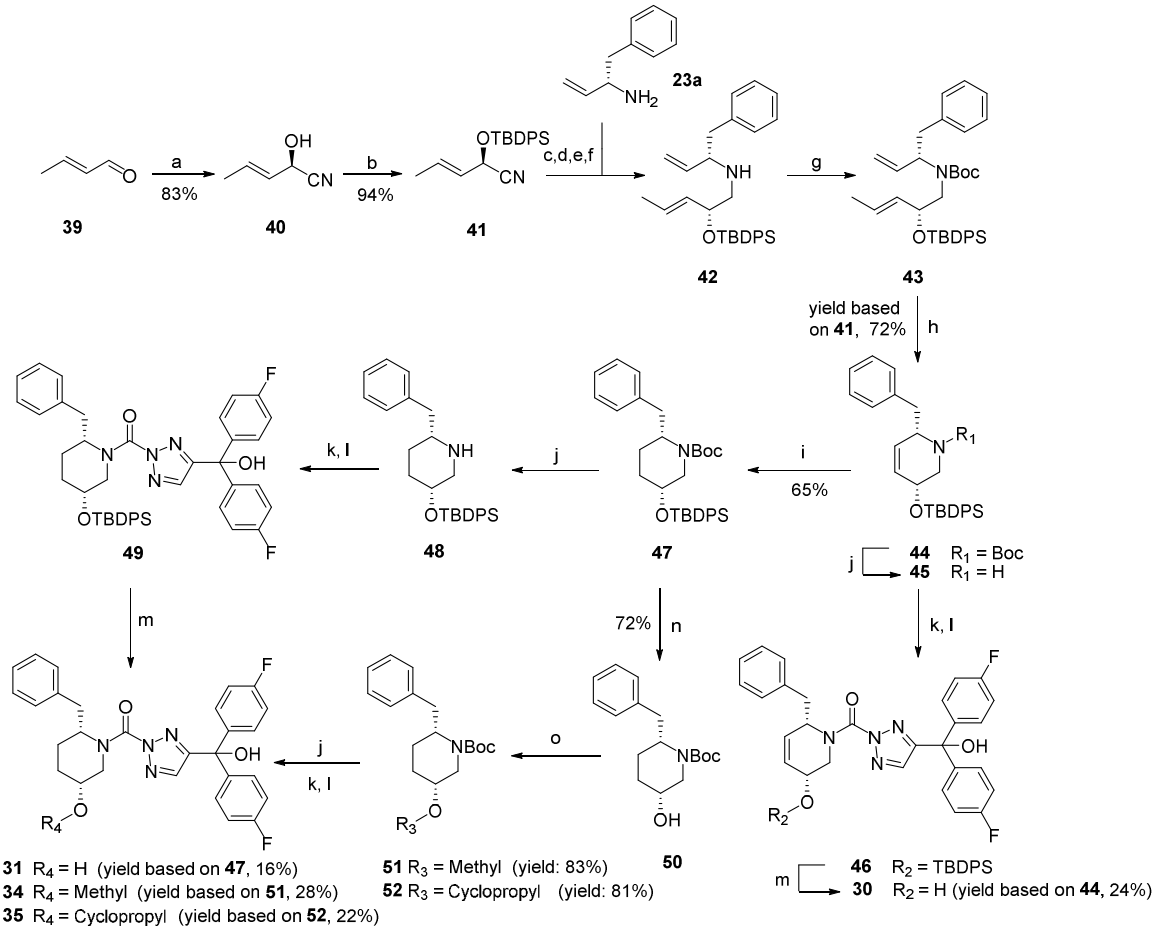

Reagents and conditions: (a) HCN, EtOAc, 0.1 M aq. citrate buffer, pH 5.4, Hydroxynitrile lyases; (b) TBDPS-Cl, imidazole, DMF, 0 ^{o}C; (c) diethyl ether, DIBAL-H, -80 ^{o}C to 0 ^{o}C; (d) MeOH, -90 ^{o}C; (e) (*S*)-amine (**23a**) (3 equiv), r.t., 20h; (f) $NaBH_4$; (g)

Boc_2O, Et_3N, THF, 50 °C, 20h; (h) Grubbs G_1 cat. 4 mol%, DCM, reflux, 48h; (i) Hydrazine, $CuSO_4$, EtOH, 0 °C to 70 °C; (j) 25% TFA, DCM, r.t.; (k) DIPEA, triphosgene, THF, 0 °C; (l) DIPEA, DMAP, triazole, THF, 60 °C; (m) HF-Pyridine, THF : pyridine = 1:1 (v/v); (n) TBAF, THF, r.t.; (o) NaH, corresponding bromide.

Table 2. Structure-activity relationship of N2-triazole urea isomers with functionalized chiral pure (2-benzyl)-piperidine staying groups

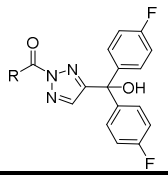

Entry	R	pIC_{50}± SEM (DAGLα)	pIC_{50}± SEM (ABHD6)	Entry	R	pIC_{50}± SEM (DAGLα)	pIC_{50}± SEM (ABHD6)
30	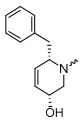	7.9±0.1	7.4±0.1	**35**	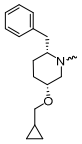	9.2±0.1	7.4±0.1
31	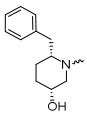	7.7±0.1	6.8±0.1	**36**	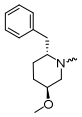	8.1±0.1	6.9±0.2
32	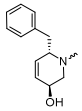	7.7±0.1	6.6±0.1	**37**	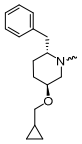	7.7±0.1	5.6±0.1
33	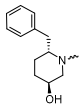	5.2±0.1	6.7±0.2	**38**	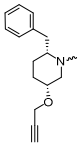	8.9±0.1	8.6±0.2
34	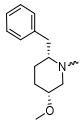	9.1±0.1	7.3±0.1				

Activity and selectivity on endogenous DAGLα and ABHD6 in brain membrane proteome.

To determine the activity and selectivity of our inhibitors in native proteomes, we incubated the most potent chiral inhibitors **34-38** for 30 min with mouse brain membrane homogenates and performed a gel-based ABPP-assay using ABPs MB064 and FP-TAMRA. All compounds block DAGLα labeling in a concentration dependent manner. Complete blockade of DAGLα was already observed at 10 nM for compounds **34**, **35** and **38**, whereas the diastereoisomers **36** and **37** were less active (Figure 3b and Figure S.3). Compound **35** inhibited labeling of DAGLα and ABHD6 with pIC_{50} of 8.7±0.1 and 6.5±0.1, respectively. This indicated that **35** is ~160-fold selective over ABHD6 (Figure 3c). Of note, compound **38** showed ~126 fold selectivity over ABHD6. No additional off-targets were identified using FP-TAMRA as a probe (Figure S.4).

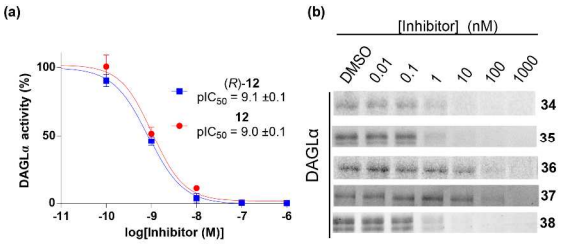

(c)

pIC_{50} ABPP(MB064)	34	35	36	37	38
DAGLα	8.7±0.1	8.7±0.1	7.1±0.1	7.1±0.1	9.2±0.1
ABHD6	7.3±0.1	6.5±0.1	6.4±0.1	<5	7.1±0.1
Selectivity fold	~25	~160	~5	~145	~126

Figure 3. (a) Concentration-dependent inhibition of hDAGLα by **12** and **(*R*)-12** as measured with a colorimetric assay based on the hydrolysis of PNP butyrate; Data represent average values ± SEM; n = 4 per group. (b) Representative fluorescent gel-based competitive ABPP with **34-38** in mouse brain proteome by activity-based probe

MB064 (0.25 μM, 30 min). (c) pIC_{50} ± SEM and selectivity of compounds **34-38** against DAGLα and ABHD6 as determined by competitive ABPP (n=3 per group).

***In vivo* efficacy of compound 38**.

Activation of the cannabinoid CB_1 receptor is a clinically proven signalling pathway controlling the energy balance in humans.[22] Rimonabant, a cannabinoid CB_1 receptor inverse agonist reduced body weight and waist circumference in obese patients and improved cardiovascular risk factors, possibly via reducing food intake and increasing energy expenditure through activation of thermogenic brown adipose tissue.[23] DAGLα knockout mice have shown hypophagia and leanness similar to that of cannabinoid CB_1 receptor knockout mice, while mice in which the gene for DAGLβ is disrupted do not share this phenotype.[24] Fasting-induced refeeding of mice is a typical CB_1-receptor mediated behaviour that is accompanied by increased 2-AG levels in the hypothalamus and can be prevented by pre-treatment with rimonabant.[25] Since we have previously shown that compound **38** is able to reduce brain levels of 2-AG in a dose- and time dependent manner [15], we set out to test whether compound **38** could also inhibit fasting-induced refeeding. Based on our previous *in vivo* results with compound **38**, we have chosen a dose of 50 mg/kg, because this leads to complete DAGL inhibition for more than 4h.[15] Mice were fasted for 18h and received a single intraperitoneal injection of vehicle (saline/ethanol/PEG40 (18:1:1; v/v/v)) or compound **38** (50 mg/kg) 30 min before refeeding, and cumulative food intake was measured up to 16h. Within 2h, compound **38**-treated mice only consumed a third of the food compared to the vehicle-treated mice, and the effect of reduction in food-take maintained up to 4h (Figure 4a). After 16h, however, food intake in compound **38**-treated mice was back to the

same levels as in vehicle-treated mice (Figure S.5), which paralleled the recovery of brain 2-AG levels. Consistent with the delay in refeeding of compound **38**-treated mice, indirect calorimetric measurements indicated that carbohydrate and fat oxidation remained respectively low and high for a prolonged period (Figure 4b-c). Importantly, compound **38**-treated mice showed no effect on locomotor activity (Figure 4d, over 4h; Figure S.5, over 24h) as measured by infrared beam breaks in Y and Z planes. Altogether, these results support the notion that DAGLα regulates food intake.

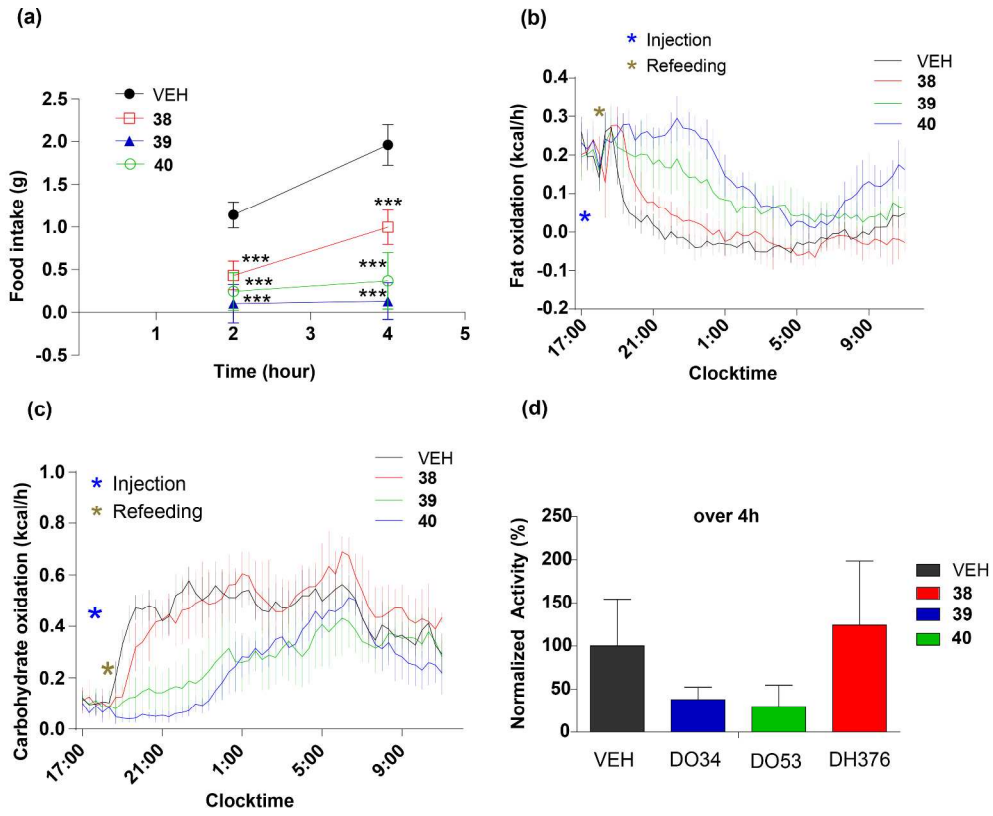

Figure. 4 (a-d) *In vivo* effects of DAGL inhibitors **38**, **39** and control compound **40** on food intake (a), fat/carbohydrate oxidation (b, c) and locomotor activity (d, 0-4h) in mice. Cumulative food intake was measured in 18h fasted mice. The animals received a single intraperitoneal injection of vehicle (black), or **38** (red), **39** (blue), and **40** (green) (50 mg/kg) 30 min before the start of refeeding and the testing period. The fat and carbohydrate oxidation of the animals were calculated from the $V \cdot O_2$ and $V \cdot CO_2$ in metabolic cages (in 20 min bins), and the locomotor activity over 4h of the animals was measured by infrared beam breaks in Y and Z axis. Data represent average values ± SEM; n = 8 mice per group. $^{**}P < 0.01$; $^{***}P < 0.001$ for all groups vs. the vehicle-treated group.

Previously, we have reported another centrally active DAGL inhibitor **39** and a structurally related control probe **40** (DO53)[15] (structures are shown in Supporting Information, Figure S.6). Compound **39** reduced brain 2-AG levels in dose- and time dependent manner, whereas the control probe **40** did not affect brain 2-AG levels. Therefore, we examined the effects of **39** and **40** on fasting-induced refeeding, indirect calorimetry and locomotor activity and observed that food intake was completely blocked in **39**-treated mice, which was again also reflected by the calorimetric measurements. Surprisingly, control probe **40**-treated mice also showed significant reductions in fasting-induced refeeding, and both **39**- and **40**-treated mice were hypolocomotive (Figure 4). These data suggest that there are one or more off-targets shared by the DAGL inhibitors (**38** and **39**) and control probe **40** that may also be involved in controlling food intake in fasting-induced mice. For example, carboxylesterase was identified by *ex vivo*

competitive ABPP in mouse liver as a major off-target shared by all three compounds (Figure S.7).

CONCLUSION

Here, we described the enantioselective synthesis and structure-activity-relationship (SAR) studies of 2,4-regioisomer of 1,2,3-triazole ureas as a novel chemotype of DAGLα inhibitors. We found that (*R*)-benzylpiperidine substituted triazole ureas constitute the active enantiomer for DAGLα inhibition as measured in biochemical assays and activity-based protein profiling. We showed that **29a** is a potent DAGLα inhibitor. Our investigations culminated in the discovery of compound **38**, which is a CNS-active DAGL inhibitor. We found that DAGL inhibitors **38** and **39** prevented fasting-induced refeeding of mice, which is typical cannabinoid CB_1-receptor mediated behaviour. Importantly, compound **38** did not affect locomotion. These effects are in line with the phenotypes observed with DAGLα and CB_1 receptor knockout mice. Our results also stress the importance of using negative control compounds, because compound **40** (that is a triazole urea which does not inhibit DAGL) also reduced food intake and did affect locomotion activity, which indicated that the triazole ureas may affect the energy balance and locomotion in mice through multiple, yet to be discovered, molecular targets.

EXPERIMENTAL SECTION

Experimental Procedures: Biochemistry.

Cloning Procedures. For the preparation of the different constructs, full length human cDNA was purchased from Source Bioscience and cloned into mammalian expression

vector pcDNA3.1, containing genes for ampicillin and neomycin resistance. DAGLα and ABHD6 constructs were obtained as reported previously.[10, 15] Plasmids were isolated from transformed XL-10 Z-competent cells (Maxi Prep, Qiagen) and verified by Sanger sequencing (BaseClear). The sequences were confirmed by sequence analysis at the Leiden Genome Technology Centre.

Cell culture and membrane preparation. Cell culture was performed as previously reported. [15] In brief, HEK293T cells were grown in DMEM with stable glutamine and phenolred (PAA or Sigma) with 10% New Born Calf serum, penicillin and streptomycin. Cells were passaged every 2-3 days by resuspending in medium and seeding them to appropriate confluence. Membranes were prepared from transiently transfected HEK293T cells. One day prior to transfection 10^7 cells were seeded in a 15 cm petri dish. Cells were transfected by the addition of a 3:1 mixture of polyethyleneimine (60 μg) and plasmid DNA (20 μg) in 2 mL serum free medium. The medium was refreshed after 24h, and after 72h the cells were harvested by suspending them in 20 mL medium. The suspension was centrifuged for 10 min at 1000 rpm, and the supernatant was removed. The cell pellet was stored at -80 ^{o}C until use.

Cell pellets were thawed on ice and suspended in lysis buffer A (20 mM HEPES, 2 mM DTT, 0.25 M sucrose, 1 mM $MgCl_2$, 1x Cocktail (Roche cOmplete EDTA free), 25 U/mL Benzonase). The suspension was homogenized by polytrone (3 × 7 sec) and incubated for 30 min on ice. The suspension was subjected to ultracentrifugation (93,000 × g, 30 min, 4 ^{o}C, Beckman Coulter, Type Ti70 rotor) to yield the cytosolic fraction in the supernatant and the membrane fraction as a pellet. The pellet was resuspended in lysis buffer B (20 mM HEPES, 2 mM DTT, 1x Cocktail (Roche cOmplete EDTA free)). The

protein concentration was determined with Quick Start Bradford reagent (BioRad) or Qubit™ fluorometric quantitation (Life Technologies). The protein fractions were diluted to a total protein concentration of 1 mg/mL and stored in small aliquots at -80 °C until use.

Biochemical DAGL activity assay. The biochemical hDAGLα assay was performed as reported previously. [10] In brief, the biochemical hDAGLα activity assay is based on the hydrolysis of *para*-nitrophenylbutyrate (PNP-butyrate) by membrane preparations from HEK293T cells transiently transfected with hDAGLα. Reactions were performed in 50 mM pH 7.2 HEPES buffer with 0.05 μg/μL final protein concentration hDAGLα transfected protein.

Natural substrate based fluorescence assay (DAGLα and ABHD6). The natural substrate assay was performed as reported previously [11, 19]. Standard assay conditions: 0.2 U/mL glycerol kinase (GK), glycerol-3-phosphate oxidase (GPO) and horseradish peroxidase (HRP), 0.125 mM ATP, 10 μM Amplifu™Red, 5% DMSO in a total volume of 200 μL. For ABHD6, the assay additionally contained 25 μM 2-AG and 0.5% acetonitrile, with a final protein concentration of 40 μg/mL. For DAGLα, the assay additionally contained 5 μg/mL MAGL-overexpressing membranes, 100 μM SAG and 0.0075% (w/v) Triton X-100, with a final protein concentration of 50 μg/mL.

Preparation of mouse brain membrane proteome. Mouse brain membrane proteome preparation was performed as previously reported. [15] In brief, mouse brains were isolated according to guidelines approved by the ethical committee of Leiden University (DEC#10095). Mouse brains were Dounce homogenized in pH 7.2 lysis buffer A (20 mM

HEPES pH 7.2, 2 mM DTT, 1 mM $MgCl_2$, 25 U/mL Benzonase) and incubated for 5 min on ice, followed by low speed spin (2,500 × g, 3 min, 4 ^oC) to remove debris. The supernatant was subjected to ultracentrifugation (100,000 × g, 45 min, 4 ^oC, Beckman Coulter, Type Ti70 rotor) to yield the cytosolic fraction in the supernatant and the membrane fraction as a pellet. The pellet was resuspended in storage buffer B (20 mM HEPES pH 7.2, 2 mM DTT). The total protein concentration was determined with Quick Start Bradford reagent (Bio-Rad) or Qubit^{TM} fluorometric quantitation (Life Technologies). Membranes and supernatant were flash frozen in liquid nitrogen and stored in aliquots at -80 ^oC until use.

Activity based protein profiling in mouse brain. Mouse brain proteome (2 mg/mL, 19.5 µL) was incubated with DMSO or inhibitor in 0.5 µL DMSO for 30 min at r.t. and subsequently incubated with 250 nM (final concentration) ABP MB064, or 500 nM (final concentration) ABP TAMRA-FP for 20 min at r.t. before the reaction was quenched with standard 3x Laemmli sample buffer. The gels were scanned using a ChemiDoc MP system and analyzed using Image Lab 4.1.

ABPP inhibitor activity measurements. The percentage of activity remaining was determined by measuring the integrated optical intensity of the fluorescent protein bands using Image Lab 4.1. The relative intensity was compared to the vehicle-treated proteins, which were set to 100%. IC_{50} values were determined by plotting a log (inhibitor) vs. normalized response (Variable slope) dose-response curve generated using Prism software (Graphpad Prism 5.0).

***In vivo* studies with 38, 39 and 40.** All animal experiments were approved by the Ethics Committee on Animal Care and Experimentation of the Leiden University Medical Center. 12-week-old male C57Bl/6J mice (Charles River, Saint-Germain-Nuelles, France) were single housed in metabolic cages (LabMaster System, TSE Systems, Bad Homburg, Germany) with a regular 12:12h light/dark cycle (6 a.m.- 6 p.m.) and free access to food and water unless noted otherwise. After 3 days of acclimatization, mice were fasted for 18h starting at midnight followed by an intraperitoneal injection with **38** (50 mg/kg), **39** (50 mg/kg), **40** (50 mg/kg) or vehicle 30 min prior to refeeding. Solutions were prepared in mixture of saline/ethanol/PEG40 (18:1:1; v/v/v). Cumulative food intake, oxygen uptake ($V{\cdot}O_2$), carbon dioxide production ($V{\cdot}CO_2$) and physical activity (beam breaks) were monitored. Carbohydrate oxidation was calculated using the formula ((4.585* $V{\cdot}CO_2$)-(3.226* $V{\cdot}O_2$))*4, in which the 4 represents the conversion from mass per time unit to kcal per time unit. Similarly, fat oxidation was calculated using the formula ((1.695* $V{\cdot}O_2$)-(1.701* $V{\cdot}CO_2$))*9.

Experimental Procedures: Chemistry.

General Remarks. All reactions were performed using oven or flame-dried glassware and dry solvents. Reagents were purchased from Sigma Aldrich, Acros or Merck and used without further purification unless noted otherwise. All moisture sensitive reactions were performed under an argon atmosphere. Traces of water were removed from starting compounds by co-evaporation with toluene.

^{1}H- and ^{13}C-NMR spectra were recorded on a Bruker AV 400 MHz spectrometer at 400 (^{1}H) and 101 (^{13}C) MHz, or on a Bruker DMX-600 spectrometer 600 (^{1}H) and 150 (^{13}C) MHz using

$CDCl_3$, CD_3OD or $(CD_3)_2SO$ as solvent, unless stated otherwise. Chemical shift values are reported in ppm with tetramethylsilane or solvent resonance as the internal standard ($CDCl_3$, δ 7.26 for ^1H, δ 77.16 for ^{13}C; CD_3OD, δ 3.31 for ^1H, δ 49.00 for ^{13}C; $(CD_3)_2SO$, δ 2.50 for ^1H, δ 39.52 for ^{13}C). Data are reported as follows: chemical shifts (δ), multiplicity (s = singlet, d = doublet, dd = double doublet, td = triple doublet, t = triplet, q = quartet, m = multiplet, br = broad), coupling constants *J* (Hz), and integration. HPLC purification was performed on a preparative LC-MS system (Agilent 1200 series) with an Agilent 6130 Quadruple MS detector. High-resolution mass spectra (HRMS) were recorded on a Thermo Scientific LTQ Orbitrap XL. IR spectra were recorded on a Shimadzu FTIR-8300 and are reported in cm^{-1}. Optical rotations were measured on a Propol automatic polarimeter (Sodium D-line, λ = 589 nm). Flash chromatography was performed using SiliCycle silica gel type SilicaFlash P60 (230 – 400 mesh). TLC analysis was performed on Merck silica gel 60/Kieselguhr F254, 0.25 mm. Compounds were visualized using either Seebach's reagent (a mixture of phosphomolybdic acid (25 g), cerium (IV) sulfate (7.5 g), H_2O (500 mL) and H_2SO_4 (25 mL)) or a $KMnO_4$ stain (K_2CO_3 (40 g), $KMnO_4$ (6 g), H_2O (600 mL) and 10% NaOH (5 mL)).

Analysis of Compound Purity by LC/MS. Compound purity was determined by an LCQ Adventage Max (Thermo Finnigan) ion-trap spectrometer (ESI+) coupled to a Surveyor HPLC system (Thermo Finnigan) equipped with a C_{18} (Gemini, 4.6 mm x 50 mm, 3 μm particle size, Phenomenex) equipped with buffer A: H_2O, B: acetonitrile (MeCN) and C: 1% aqueous TFA. All final compounds were determined to be above 95% pure by this method.

(2-Benzylpiperidin-1-yl)(4-(hydroxydiphenylmethyl)-1*H*-1,2,3-triazol-1-yl)methanone (3). A solution of 2-benzylpiperidine (50.0 mg, 0.285 mmol) in THF (4 mL) was treated with DIPEA (0.249 mL, 1.426 mmol) and bis(trichloromethyl) carbonate (42.3 mg, 0.143 mmol) and

the reaction mixture was stirred for 30 min at 0 °C. The mixture was poured into water and extracted with ethyl acetate (3 x 20 mL). The organic layer was washed with water, brine, dried over $MgSO_4$, filtered and concentrated under reduced pressure. The intermediate was dissolved in a mixture of THF (8 mL) and DIPEA (0.249 mL, 1.426 mmol), DMAP (34.9 mg, 0.285 mmol) and diphenyl(1H-1,2,3-triazol-4-yl)methanol (71.7 mg, 0.285 mmol) were added to the solution. The mixture was stirred for two hours at 60 °C and poured into a saturated aqueous NH_4Cl solution. The mixture was extracted with ethyl acetate (3 x 20 mL), washed with water, brine, dried over $MgSO_4$ and filtered. The solvents were removed under reduced pressure to yield the crude triazole urea as a mixture of N1- and N2-carbamoylated regioisomers. The N1-carbamoyl triazole was isolated by silica gel chromatography (pentane/EtOAc 100:1 → 5:1) to afford 1,4-triazole urea **3** (29.7 mg, 0.066 mmol, 23% yield). HRMS [ESI+] m/z: calculated for $C_{28}H_{28}N_4O_2$ $[M+H]^+$ 453.2285, found: 453.2283. ^{1}H NMR (400 MHz, $CDCl_3$) δ 7.39 – 7.27 (m, 10H), 7.04 – 6.82 (m, 5H), 4.76 (s, 1H), 4.28 (br s, 1H), 3.71 (br s, 1H), 3.33 – 3.21 (m, 2H), 2.63 (br s, 1H), 2.00 – 1.66 (m, 6H). ^{13}C NMR (101 MHz, $CDCl_3$) δ 145.28, 137.90, 129.03, 128.78, 128.18, 127.76, 127.29, 127.23, 127.22, 126.80, 123.76, 69.63, 57.47, 40.46, 36.50, 29.18, 25.32, 18.75.

(2-Benzylpiperidin-1-yl)(4-(hydroxydiphenylmethyl)-2*H*-1,2,3-triazol-2-yl)methanone (4). The title compound was isolated from the mixture of compound **3**. The N2-carbamoyl triazole regioisomer was purified by silica gel chromatography (pentane/EtOAc 100:1 → 5:1) to afford 2,4-triazole urea **4** (39.0 mg, 0.086 mmol, 30% yield). HRMS [ESI+] m/z: calculated for $C_{28}H_{28}N_4O_2$ $[M+H]^+$ 453.2285, found: 453.2284. ^{1}H NMR (400 MHz, $CDCl_3$) δ 7.52 (s, 1H), 7.35 – 7.27 (m, 10H), 7.22 – 6.97 (m, 5H), 4.75 – 4.17 (m, 1H), 3.68 (br s, 1H), 3.26 – 3.19 (m, 1H), 3.10 – 3.15 (m, 1H), 2.93 (br s, 1H), 1.79 – 1.60 (m, 6H). ^{13}C NMR (101 MHz, $CDCl_3$) δ 155.48, 149.55, 145.04, 137.91, 135.14, 129.07, 128.64, 128.21, 127.84, 127.22, 126.64, 69.61,

53.28, 42.44, 36.31, 26.05, 25.24, 18.71.

(4-([1,1'-Biphenyl]-4-yl)-1*H*-1,2,3-triazol-1-yl)(2-ethylpiperidin-1-yl)methanone (5). The title compound was synthesized from 2-ethylpiperidine (0.059 mL, 0.442 mmol) and 4-([1,1'-biphenyl]-4-yl)-1H-1,2,3-triazole (98.0 mg, 0.442 mmol) according to the procedures described for compound **3**. The N1-carbamoyl triazole was isolated by silica gel chromatography (pentane/EtOAc 100:1 → 5:1) to afford 1,4-triazole urea **5** (48.0 mg, 0.133 mmol, 30% yield). HRMS [ESI+] m/z: calculated for $C_{22}H_{24}N_4O$ $[M+H]^+$ 361.2023, found: 361.2022. ^{1}H NMR (400 MHz, $CDCl_3$) δ 8.35 (s, 1H), 7.95 (d, *J* = 8.4 Hz, 2H), 7.69 (d, *J* = 8.4 Hz, 2H), 7.66 – 7.61 (m, 2H), 7.47 – 7.44 (m, 2H), 7.38 -7.34 (m, 1H), 4.55 (q, *J* = 6.6 Hz, 1H), 4.29 (br d, *J* = 13.4 Hz, 1H), 3.20 (br s, 1H), 1.87 – 1.66 (m, 8H), 0.94 (s, 3H). ^{13}C NMR (101 MHz, $CDCl_3$) δ 146.54, 141.42, 140.52, 128.93, 128.71, 127.70, 127.63, 127.08, 126.35, 120.95, 55.26, 53.87, 42.83, 28.15, 25.74, 22.60, 18.86, 10.70.

(4-([1,1'-Biphenyl]-4-yl)-2*H*-1,2,3-triazol-2-yl)(2-ethylpiperidin-1-yl)methanone (6). The title compound was isolated from the mixture of compound **5**. The N2-carbamoyl triazole regioisomer was isolated by silica gel chromatography (pentane/EtOAc 100:1 → 5:1) to afford 2,4-triazole urea **6** (36.0 mg, 0.100 mmol, 23% yield). HRMS [ESI+] m/z: calculated for $C_{22}H_{24}N_4O$ $[M+H]^+$ 361.2023, found: 361.2024. ^{1}H NMR (400 MHz, $CDCl_3$) δ 8.08 (s, 1H), 7.94 (d, *J* = 8.3 Hz, 2H), 7.69 (d, *J* = 8.3 Hz, 2H), 7.63 (d, *J* = 7.7 Hz, 2H), 7.46 (t, *J* = 7.6 Hz, 2H), 7.38 (t, *J* = 7.5 Hz, 1H), 4.26 (br s, 2H), 3.16 (br s, 1H), 1.88 – 1.63 (m, 8H), 0.96 (s, 3H). ^{13}C NMR (101 MHz, $CDCl_3$) δ 148.64, 142.12, 140.36, 132.95, 128.96, 128.25, 127.77, 127.70, 127.10, 126.90, 53.85, 43.21, 42.24, 28.01, 25.94, 22.78, 18.93, 10.76.

(2-Benzylpiperidin-1-yl)(4-(dicyclohexyl(hydroxy)methyl)-2*H*-1,2,3-triazol-2-

yl)methanone (7). The title compound was synthesized from 2-benzylpiperidine (73.6 mg, 0.42 mmol) and dicyclohexyl(2*H*-1,2,3-triazol-4-yl) methanol (122 mg, 0.462 mmol). According to the procedures described for compound **3**. The N2-carbamoyl triazole was isolated by silica gel chromatography (pentane/EtOAc 100:1 → 5:1) to afford 2,4-triazole urea **7** (31.0 mg, 0.067 mmol, 16% yield). HRMS [ESI+] m/z: calculated for $C_{28}H_{40}N_4O_2$ [M+H$^+$] 465.3224, found: 465.3221. ^{1}H NMR (400 MHz, $CDCl_3$) δ 7.59 (s, 1H), 7.37 – 7.04 (m, 5H), 4.59 (br s, 1H), 3.81 – 3.68 (m, 1H), 3.28 (td, *J* = 13.3, 2.9 Hz, 1H), 3.10 (dd, *J* = 13.3, 6.4 Hz, 1H), 2.99 (t, *J* = 11.6 Hz, 1H), 1.93 – 1.59 (m, 16H), 1.45 – 1.34 (m, 2H), 1.27 – 1.15 (m, 4H), 1.10 – 0.98 (m, 4H), 0.84 – 0.72 (m, 2H). ^{13}C NMR (101 MHz, $CDCl_3$) δ 153.64, 149.83, 137.99, 134.24, 129.10, 128.60, 126.64, 78.22, 67.99, 43.88, 42.45, 36.10, 29.71, 27.22, 26.52, 26.42, 26.21, 25.46, 18.78.

(2-Benzylpiperidin-1-yl)(4-(1-hydroxycyclohexyl)-2*H*-1,2,3-triazol-2-yl)methanone (8). The title compound was synthesized from 2-benzylpiperidine (88.0 mg, 0.500 mmol) and 1-(2*H*-1,2,3-triazol-4-yl)cyclohexan-1-ol (92 mg, 0.550 mmol). According to the procedures described for compound **3**. The N2-carbamoyl triazole was isolated by silica gel chromatography (pentane/EtOAc 100:1 → 5:1) to afford 2,4-triazole urea **8** (61.0 mg, 0.17 mmol, 34% yield). HRMS [ESI+] m/z: calculated for $C_{21}H_{28}N_4O_2$ [M+H$^+$] 369.2285, found: 369.2288. ^{1}H NMR (400 MHz, $CDCl_3$) δ 7.76 (s, 1H), 7.36 – 7.09 (m, 5H), 4.63 (br s, 1H), 4.14 (br s, 1H), 3.29 (td, *J* = 13.2, 2.9 Hz, 1H), 3.16 (dd, *J* = 13.3, 6.1 Hz, 1H), 3.06 – 2.98 (m, 1H), 2.29 (br s, 1H), 2.02 – 1.55 (m, 16H), 1.45 – 1.33 (m, 1H). ^{13}C NMR (101 MHz, $CDCl_3$) δ 157.07, 149.78, 138.07, 132.99, 129.11, 128.59, 126.61, 69.77, 53.47, 42.23, 38.01, 36.04, 26.62, 25.47, 25.25, 21.79, 18.78.

(2-Benzylpiperidin-1-yl)(4-(1-hydroxy-1-phenylethyl)-2*H*-1,2,3-triazol-2-yl)methanone (9). The title compound was synthesized from 2-benzylpiperidine (88.0 mg, 0.500 mmol) and 1-phenyl-1-(1*H*-1,2,3-triazol-4-yl)ethan-1-ol (104 mg, 0.550 mmol) according to the procedures described for compound **3**. The N2-carbamoyl triazole was isolated by silica gel chromatography (pentane/EtOAc 100:1 → 5:1) to afford 2,4-triazole urea **9** (25.0 mg, 0.064 mmol, 13% yield). HRMS [ESI+] m/z: calculated for $C_{23}H_{26}N_4O_2$ [M+H$^+$] 391.2129, found: 391.2131. ^{1}H NMR (400 MHz, $CDCl_3$) δ 7.66 (d, *J* = 3.5 Hz, 1H), 7.53 – 7.46 (m, 2H), 7.42 – 7.34 (m, 2H), 7.34 – 7.30 (m, 1H), 7.29 – 7.17 (m, 5H), 4.76 – 4.31 (m, 2H), 3.30 (td, *J* = 13.4, 2.8 Hz, 1H), 3.15 (dd, *J* = 13.3, 6.2 Hz, 1H), 3.08 – 2.95 (m, 1H), 2.86 (br s, 1H), 2.02 (d, *J* = 2.5 Hz, 3H), 1.90 – 1.57 (m, 6H). ^{13}C NMR (101 MHz, $CDCl_3$) δ 145.82, 138.03, 133.69, 129.12, 128.66, 128.45, 127.57, 126.67, 125.15, 72.39, 63.05, 35.57, 30.64, 25.48, 18.81.

(2-Benzylpiperidin-1-yl)(4-(2-hydroxypropan-2-yl)-2*H*-1,2,3-triazol-2-yl)methanone (10). The title compound was synthesized from 2-benzylpiperidine (88.0 mg, 0.500 mmol) and 2-(2*H*-1,2,3-triazol-4-yl)propan-2-ol (69.9 mg, 0.550 mmol) according to the procedures described for compound **3**. The N2-carbamoyl triazole was isolated by silica gel chromatography (pentane/EtOAc 100:1 → 5:1) to afford 2,4-triazole urea **10** (17.0 mg, 0.052 mmol, 11% yield). HRMS [ESI+] m/z: calculated for $C_{18}H_{24}N_4O_2$ [M+H$^+$] 329.1972, found: 329.1971. ^{1}H NMR (400 MHz, $CDCl_3$) δ 7.76 (s, 1H), 7.43 – 6.95 (m, 5H), 4.65 (br s, 1H), 4.37 – 3.94 (m, 1H), 3.49 (br s, 1H), 3.30 (td, *J* = 13.3, 2.8 Hz, 1H), 3.16 (br s, 1H), 3.06 – 2.98 (m, 1H), 1.89 – 1.61 (m, 12H). ^{13}C NMR (101 MHz, $CDCl_3$) δ 157.12, 149.78, 138.03, 132.74, 129.09, 128.62, 126.57, 68.82, 55.06, 42.43, 36.02, 30.31, 25.42, 18.83.

(2-Benzylpiperidin-1-yl)(4-(hydroxydi(pyridin-2-yl)methyl)-2*H*-1,2,3-triazol-2-yl)methanone (11). The title compound was synthesized from 2-benzylpiperidine (59.6 mg,

0.340 mmol) and di(pyridin-2-yl)(1*H*-1,2,3-triazol-4-yl)methanol (95.0 mg, 0.374 mmol) according to the procedures described for compound **3**. The N2-carbamoyl triazole was isolated by silica gel chromatography (pentane/EtOAc 100:1 → 5:1) to afford 2,4-triazole urea **11** (30 mg, 0.066 mmol, 19% yield). HRMS [ESI+] m/z: calculated for $C_{26}H_{26}N_6O_2$ $[M+H]^+$ 455.2190, found: 455.2186. ^{1}H NMR (400 MHz, $CDCl_3$) δ 8.66 (br d, *J* = 4.4 Hz, 2H), 8.43 (br s, 2H), 8.02 – 7.90 (m, 4H), 7.48 – 7.45 (m, 2H), 7.24 – 6.95 (m, 4H), 4.70 – 3.80 (m, 2H), 3.23 (td, *J* = 13.5, 2.6 Hz, 1H), 3.07 (dd, *J* = 13.1, 6.3 Hz, 1H), 2.96 (br s, 1H), 1.79 – 1.61 (m, 6H). ^{13}C NMR (101 MHz, $CDCl_3$) δ 158.82, 152.26, 149.47, 145.84, 140.26, 137.96, 135.16, 129.20, 128.68, 126.69, 124.42, 123.99, 76.10, 56.46, 45.37, 36.00, 25.57, 25.47, 18.79.

(2-Benzylpiperidin-1-yl)(4-(bis(4-fluorophenyl)(hydroxy)methyl)-2*H*-1,2,3-triazol-2-yl)methanone (12). The title compound was synthesized from 2-benzylpiperidine (100 mg, 0.571 mmol) and bis(4-fluorophenyl)(1*H*-1,2,3-triazol-4-yl)methanol (164 mg, 0.571 mmol) according to the procedures described for compound **3**. The N2-carbamoyl triazole was isolated by silica gel chromatography (pentane/EtOAc 100:1 → 5:1) to afford 2,4-triazole urea **12** (71.0 mg, 0.145 mmol, 26% yield). HRMS [ESI+] m/z: calculated for $C_{28}H_{26}F_2N_4O_2$ $[M+H]^+$ 489.2097, found: 489.2097. ^{1}H NMR (400 MHz, $CDCl_3$) δ 7.51 (s, 1H), 7.34 – 7.24 (m, 5H), 7.18 (br, 3H), 7.02 – 6.97 (m, 5H), 4.47 – 4.26 (m, 1H), 3.80 (br s, 1H), 3.28 – 3.21 (m, 1H), 3.08 (dd, *J* = 13.2, 6.5 Hz, 1H), 2.94 (br s, 1H), 1.77 – 1.63 (m, 6H). ^{13}C NMR (101 MHz, $CDCl_3$) δ 162.35 (d, *J* = 248.5 Hz), 155.29, 149.47, 140.84, 137.91, 134.89, 131.03, 129.08 (d, *J* = 8.1 Hz), 128.69, 126.75, 115.15 (d, *J* = 21.2 Hz), 76.50, 56.81, 43.26, 36.12, 25.56, 25.55, 18.88.

(2-Benzylpiperidin-1-yl)(4-(bis(4-fluorophenyl)(methoxy)methyl)-2*H*-1,2,3-triazol-2-yl)methanone (13). The title compound was synthesized from 2-benzylpiperidine (50.8 mg, 0.290 mmol) and 4-(bis(4-fluorophenyl)(methoxy)methyl)-1H-1,2,3-triazole (96.0 mg, 0.319

mmol) according to the procedures described for compound **3**. The N2-carbamoyl triazole was isolated by silica gel chromatography (pentane/EtOAc 100:1 → 5:1) to afford 2,4-triazole urea **13** (13.0 mg, 0.025 mmol, 10% yield). HRMS [ESI+] m/z: calculated for $C_{29}H_{28}F_2N_4O_2$ $[M+Na]^+$ 525.2073, found: 525.2069. ^{1}H NMR (400 MHz, $CDCl_3$) δ 7.61 (s, 1H), 7.49 – 7.39 (m, 4H), 7.32 – 7.15 (m, 5H), 7.03 (td, *J* = 8.6, 1.5 Hz, 4H), 4.73 (br s, 1H), 4.39 (br s, 1H), 3.28 (td, *J* = 13.3, 2.9 Hz, 1H), 3.18 (s, 3H), 3.10 (dd, *J* = 13.2, 6.4 Hz, 1H), 3.04 – 2.94 (m, 1H), 1.85 – 1.56 (m, 6H). ^{13}C NMR (101 MHz, $CDCl_3$) δ 162.14 (d, *J* = 247.2 Hz), 152.51, 149.48, 138.30, 137.87, 135.89, 129.68 (d, *J* = 13.0 Hz), 129.11, 128.59, 126.63, 115.07 (d, *J* = 21.4 Hz), 81.60, 54.56, 52.45, 43.32, 36.21, 26.40, 25.42, 18.72.

(4-(Hydroxydiphenylmethyl)-2*H*-1,2,3-triazol-2-yl)(2-(phenoxymethyl)piperidin-1-yl)methanone (14). The title compound was synthesized from 2-(phenoxymethyl)piperidine (60.0 mg, 0.314 mmol) and diphenyl(1*H*-1,2,3-triazol-4-yl)methanol (87.0 mg, 0.345 mmol) according to the procedures described for compound **3**. The N2-carbamoyl triazole was isolated by silica gel chromatography (pentane/EtOAc 100:1 → 5:1) to afford 2,4-triazole urea **14** (36.7 mg, 0.078 mmol, 25 % yield). HRMS [ESI+] m/z: calculated for $C_{28}H_{28}N_4O_3$ $[M+H]^+$ 469.2234, found: 469.2233. ^{1}H NMR (400 MHz, $CDCl_3$) δ 7.56 (s, 1H), 7.34 – 7.21 (m, 12H), 6.94 (t, *J* = 7.4 Hz, 1H), 6.84 (br d, *J* = 8.0 Hz, 2H), 4.74 (br s, 1H), 4.26 – 4.22 (m, 1H), 4.06 (br s, 1H), 3.54 (br s, 1H), 3.15 (br s, 1H), 1.91 – 1.85 (m, 2H), 1.79 – 1.63 (m, 4H). ^{13}C NMR (101 MHz, $CDCl_3$) δ 158.33, 155.75, 150.53, 144.98, 135.39, 129.62, 128.27, 127.91, 127.26, 121.27, 114.70, 77.33, 65.77, 53.87, 41.89, 25.45, 25.11, 19.46.

(4-(Bis(4-fluorophenyl)(hydroxy)methyl)-2*H*-1,2,3-triazol-2-yl)(2-(phenoxymethyl)piperidin-1-yl)methanone (15). The title compound was synthesized from 2-(phenoxymethyl)piperidine (60.0 mg, 0.314 mmol) and bis(4-fluorophenyl)(1*H*-1,2,3-triazol-4-

yl)methanol (99.0 mg, 0.345 mmol) according to the procedures described for compound **3**. The N2-carbamoyl triazole was isolated by silica gel chromatography (pentane/EtOAc 100:1 → 5:1) to afford 2,4-triazole urea **15** (71.0 mg, 0.141 mmol, 45% yield). HRMS [ESI+] m/z: calculated for $C_{28}H_{26}F_2N_4O_3$ $[M+H]^+$ 505.2046, found: 505.2046. ^{1}H NMR (400 MHz, $CDCl_3$) δ 7.55 (s, 1H), 7.30 – 7.21 (m, 6H), 6.98 – 6.92 (m, 5H), 6.82 (br d, *J* = 8.0 Hz, 2H), 4.70 (br s, 1H), 4.26 – 4.22 (m, 1H), 4.05 (br s, 1H), 3.76 (br s, 1H), 3.14 (br s, 1H), 1.93 – 1.59 (m, 6H). ^{13}C NMR (101 MHz, $CDCl_3$) δ 162.32 (d, *J* = 248.5 Hz), 158.25, 155.52, 150.42, 140.78 (d, *J* = 10.1 Hz), 135.11, 129.57, 129.10 (d, *J* = 9.1 Hz), 121.35, 115.13 (d, *J* = 21.2 Hz), 114.63, 76.51, 65.65, 53.83, 41.99, 25.45, 25.07, 19.42.

(2-((4-Fluorophenoxy)methyl)piperidin-1-yl)(4-(hydroxydiphenylmethyl)-2*H*-1,2,3-triazol-2-yl)methanone (16). The title compound was synthesized from 2-((4-fluorophenoxy)methyl)piperidine (60.0 mg, 0.287 mmol) and diphenyl(1*H*-1,2,3-triazol-4-yl)methanol (79.0 mg, 0.315 mmol) according to the procedures described for compound **3**. The N2-carbamoyl triazole was isolated by silica gel chromatography (pentane/EtOAc 100:1 → 5:1) to afford 2,4-triazole urea **16** (27.9 mg, 0.057 mmol, 20% yield). HRMS [ESI+] m/z: calculated for $C_{28}H_{27}FN_4O_3$ $[M+H]^+$ 487.2140, found: 487.2140. ^{1}H NMR (400 MHz, $CDCl_3$) δ 7.58 (s, 1H), 7.32 – 7.27 (m, 11H), 6.90 (t, *J* = 8.4 Hz, 2H), 6.77 (br s, 1H), 4.71 (br s, 1H), 4.28 – 4.13 (m, 1H), 4.01 (br s, 2H), 3.13 (br s, 1H), 1.91 – 1.85 (m, 2H), 1.75 – 1.64 (m, 4H). ^{13}C NMR (101 MHz, $CDCl_3$) δ 157.53 (d, *J* = 239.4 Hz), 155.83, 154.42, 150.56, 145.10, 135.41, 128.23, 127.87, 127.35 (d, *J* = 22.2 Hz), 115.99, 115.73 (d, *J* = 8.1 Hz), 77.28, 66.42, 53.87, 42.94, 25.36, 25.05, 19.42.

(4-(Bis(4-fluorophenyl)(hydroxy)methyl)-2*H*-1,2,3-triazol-2-yl)(2-((4-fluorophenoxy)methyl)piperidin-1-yl)methanone (17). The title compound was synthesized

from 2-((4-fluorophenoxy)methyl)piperidine (60.0 mg, 0.287 mmol) and bis(4-fluorophenyl)(1*H*-1,2,3-triazol-4-yl)methanol (82.0 mg, 0.287 mmol) according to the procedures described for compound **3**. The N2-carbamoyl triazole was isolated by silica gel chromatography (pentane/EtOAc 100:1 → 5:1) to afford 2,4-triazole urea **17** (30.3 mg, 0.058 mmol, 20% yield). HRMS [ESI+] m/z: calculated for $C_{28}H_{25}F_3N_4O_3$ $[M+H]^+$ 523.1952, found: 523.1952. ^{1}H NMR (400 MHz, $CDCl_3$) δ 7.56 (s, 1H), 7.30 – 7.26 (m, 5H), 6.99 – 6.89 (m, 6H), 6.76 (br s, 1H), 4.69 (br s, 1H), 4.23 – 4.18 (m, 1H), 4.01 (br s, 2H), 3.79 (br s, 1H), 3.13 (t, *J* = 11.8 Hz, 1H), 1.88 – 1.65 (m, 6H). ^{13}C NMR (101 MHz, $CDCl_3$) δ 162.36 (d, *J* = 247.5 Hz), 157.59 (d, *J* = 240.4 Hz), 155.58, 154.41, 150.47, 140.8 (d, *J* = 9.0 Hz), 135.13, 129.08 (d, *J* = 8.1 Hz), 115.94 (d, *J* = 23.2 Hz), 115.71 (d, *J* = 8.1 Hz), 115.1 (d, *J* = 22.2 Hz), 76.54, 66.42, 53.07, 43.12, 25.39, 25.05, 19.42.

(4-(Bis(4-fluorophenyl)(hydroxy)methyl)-2*H*-1,2,3-triazol-2-yl)(2-(3-methoxybenzyl)piperidin-1-yl)methanone (18). The title compound was synthesized from 2-(3-methoxybenzyl)piperidine (130 mg, 0.634 mmol) and bis(4-fluorophenyl)(1*H*-1,2,3-triazol-4-yl)methanol (200 mg, 0.697 mmol) according to the procedures described for compound **3**. The N2-carbamoyl triazole was isolated by silica gel chromatography (pentane/EtOAc 100:1 → 5:1) to afford 2,4-triazole urea **18** (118 mg, 0.227 mmol, 36% yield). HRMS [ESI+] m/z: calculated for $C_{29}H_{28}F_2N_4O_3$ $[M+H]^+$ 519.2202, found: 519.2204. ^{1}H NMR (500 MHz, $CDCl_3$) δ 7.47 (s, 1H), 7.31 – 7.25 (m, 5H), 7.13 (br s, 1H), 7.04 – 6.98 (m, 5H), 6.72 (d, *J* = 8.0 Hz, 1H), 3.73 (s, 3H), 3.67 (br s, 1H), 3.49 (br s, 2H), 3.25 (t, *J* = 13.2 Hz, 1H), 3.07 (dd, *J* = 13.2, 6.7 Hz, 1H), 2.91 (br s, 1H), 1.82 – 1.57 (m, 6H). ^{13}C NMR (126 MHz, $CDCl_3$) δ 162.42 (d, *J* = 248.2 Hz), 159.78, 155.32, 149.57, 140.85, 139.46, 134.95, 129.72, 129.11 (d, *J* = 7.6 Hz), 121.49, 115.21 (d, *J* = 21.4 Hz), 112.48, 111.80, 76.51, 57.52, 55.27, 41.10, 36.24, 28.99, 25.51, 18.83.

(4-(Bis(4-fluorophenyl)(hydroxy)methyl)-2*H*-1,2,3-triazol-2-yl)(2-(4-methoxybenzyl)piperidin-1-yl)methanone (19). The title compound was synthesized from 2-(4-methoxybenzyl)piperidine (92 mg, 0.448 mmol) and bis(4-fluorophenyl)(1*H*-1,2,3-triazol-4-yl)methanol (142 mg, 0.493 mmol) according to the procedures described for compound **3**. The N2-carbamoyl triazole was isolated by silica gel chromatography (pentane/EtOAc 100:1 → 5:1) to afford 2,4-triazole urea **19** (116 mg, 0.224 mmol, 30% yield). HRMS [ESI+] m/z: calculated for $C_{29}H_{28}F_2N_4O_3$ $[M+H]^+$ 519.2202, found: 519.2199. ^{1}H NMR (500 MHz, $CDCl_3$) δ 7.48 (s, 1H), 7.32 – 7.24 (m, 5H), 7.06 – 6.97 (m, 5H), 6.74 (br s, 2H), 4.37 (br s, 2H), 3.75 (s, 3H), 3.24 (td, *J* = 13.4, 2.6 Hz, 1H), 3.03 (dd, *J* = 13.5, 6.6 Hz, 1H), 2.89 (br s, 1H), 2.43 (br s, 1H), 1.86 – 1.57 (m, 6H).^{13}C NMR (126 MHz, $CDCl_3$) δ 162.47 (d, *J* = 248.2 Hz), 158.45, 155.27, 149.53, 140.85, 134.87, 130.11, 129.93, 129.14 (d, *J* = 7.56 Hz), 115.27 (d, *J* = 21.42 Hz), 114.17, 76.58, 55.33, 51.04, 40.78, 35.33, 26.24, 25.55, 18.83.

(*(3R,6S)*-6-Benzyl-3-hydroxy-3,6-dihydropyridin-1(2H)-yl)(4-(bis(4-fluorophenyl)(hydroxy)methyl)-2*H*-1,2,3-triazol-2-yl)methanone (30). The title compound was synthesized from (*3R,6S*)-6-benzyl-3-((tert-butyldiphenylsilyl)oxy)-1,2,3,6-tetrahydropyridine (120 mg, 0.281 mmol) and bis(4-fluorophenyl)(1*H*-1,2,3-triazol-4-yl)methanol (89.0 mg, 0.309 mmol) according to the procedures described for compound **3**. The N2-carbamoyl triazole urea was isolated by silica gel chromatography (pentane/EtOAc 100:1 → 8:1). HF-Pyridine (1.55 mL, 1.70 mmol) was subsequently added to a solution of N2-carbamoyl triazole urea in THF and pyridine (1:1) with ice cooling, and the reaction mixture was stirred overnight at room temperature. The mixture was diluted with ethyl acetate (40 eq.), and then washed with $NaHCO_3$, brine, dried with $MgSO_4$, and concentrated under reduced pressure. Purified by flash chromatography to furnish the title compound **30** (34.2 mg, 0.068 mmol, 24%

yield for four steps). HRMS [ESI+] m/z: calculated for $C_{28}H_{24}F_2N_4O_3$ $[M+H]^+$ 503.1889, found: 503.1889. $[\alpha]_D^{20}$ = 245 (*c* = 0.1, $CHCl_3$). ^{1}H NMR (400 MHz, $CDCl_3$) δ 7.59 (s, 1H), 7.32 – 7.24 (m, 9H), 7.05 – 6.98 (m, 4H), 5.84 (br d, *J* = 10.4 Hz, 1H), 5.64 (br s, 1H), 4.79 (br s, 1H), 4.49 (br s, 1H), 3.25 (s, 4H), 2.95 (t, *J* = 8.0 Hz, 1H), 2.88 (br s, 1H). ^{13}C NMR (101 MHz, $CDCl_3$) δ 162.51 (d, *J* = 248.5 Hz), 156.03, 149.01, 140.63, 136.67, 135.68, 130.76, 129.54, 129.12 (d, *J* = 8.1 Hz), 128.77, 128.20, 127.10, 115.38 (d, *J* = 22.2 Hz), 76.65, 63.99, 55.62, 47.98, 38.94.

((*2R,5R*)-2-Benzyl-5-hydroxypiperidin-1-yl)(4-(bis(4-fluorophenyl)(hydroxy)methyl)-2*H*-1,2,3-triazol-2-yl)methanone (31). The title compound was synthesized *(2R,5R)*-2-benzyl-5-((tert-butyldiphenylsilyl)oxy)piperidine (80.0 mg, 0.186 mmol), bis(4-fluorophenyl)(1*H*-1,2,3-triazol-4-yl)methanol (58.8 mg, 0.205 mmol) and HF-Pyridine (0.612 mL, 0.673 mmol) according to the procedures described for compound **30**. This furnished N2-carbamoyl triazole urea ((*2R,5R)*-2-benzyl-5-hydroxypiperidin-1-yl)(4-(bis(4-fluorophenyl)(hydroxy)methyl)-2*H*-1,2,3-triazol-2-yl)methanone **31** (13.6 mg, 0.027 mmol, 16% yield). $[\alpha]_D^{20}$ = 191 (*c* = 0.1, $CHCl_3$). HRMS [ESI+] m/z: calculated for $C_{28}H_{26}F_2N_4O_3$ $[M+H]^+$ 505.2046, found: 505.2046. ^{1}H NMR (400 MHz, $CDCl_3$) δ 7.52 (s, 1H), 7.34 – 7.16 (m, 9H), 7.07 – 6.98 (m, 4H), 4.57 (br s, 1H), 4.21 (br s, 1H), 3.88 – 3.80 (m, 1H), 3.16 – 3.02 (m, 2H), 2.98 – 2.89 (m, 1H), 2.35 (br s, 2H), 2.03 – 2.00 (m, 1H), 1.79 – 1.72 (m, 3H). ^{13}C NMR (214 MHz, $CDCl_3$) δ 162.50 (d, *J* = 248.2 Hz), 155.67, 149.43, 140.68, 137.62, 135.21, 131.07, 129.16 (d, *J* = 8.6 Hz), 128.86, 126.78, 115.34 (d, *J* = 21.4 Hz), 76.62, 67.08, 53.68, 45.66, 35.89, 28.59, 27.80.

((*3S,6S*)-6-Benzyl-3-hydroxy-3,6-dihydropyridin-1(2*H*)-yl)(4-(bis(4-fluorophenyl)(hydroxy)methyl)-2*H*-1,2,3-triazol-2-yl)methanone (32). The title compound was synthesized from *(3S,6S)*-6-benzyl-3-((tert-butyldiphenylsilyl)oxy)-1,2,3,6-tetrahydropyridine (80.0 mg, 0.187 mmol), bis(4-fluorophenyl)(2*H*-1,2,3-triazol-4-yl)methanol

(59.1 mg, 0.206 mmol) and HF-pyridine (0.613 mL, 0.675 mmol) according to the procedures described for compound **30**. This furnished N2-carbamoyl triazole urea ((*3S,6S*)-6-benzyl-3-hydroxy-3,6-dihydropyridin-1(2*H*)-yl)(4-(bis(4-fluorophenyl)(hydroxy) methyl) -2*H*-1,2,3-triazol-2-yl)methanone **32** (13.9 mg, 0.028 mmol, 15% yield). $[\alpha]_D^{20}$ = 142 (*c* = 0.5, $CHCl_3$). HRMS [ESI+] m/z: calculated for $C_{28}H_{24}F_2N_4O_3$ $[M+H]^+$ 503.1889, found: 503.1888. ^{1}H NMR (400 MHz, $CDCl_3$) δ 7.58 (s, 1H), 7.45 – 7.19 (m, 9H), 7.04 – 7.00 (m, 4H), 6.03 – 5.99 (m, 1H), 5.82 (br s, 1H), 4.96 – 4.88 (m, 1H), 4.14 – 4.03 (m, 2H), 3.25 – 3.17 (m, 2H), 3.03 – 2.90 (m, 1H). ^{13}C NMR (101 MHz, $CDCl_3$) δ 162.50 (d, *J* = 248.5 Hz), 156.00, 149.43, 140.64, 136.46, 135.48, 130.05, 129.67, 129.13 (d, *J* = 8.1 Hz), 128.77, 127.12, 124.90, 115.38 (d, *J* = 22.2 Hz), 76.58, 62.51, 55.90, 48.00, 38.19.

((*2R,5S*)-2-Benzyl-5-hydroxypiperidin-1-yl)(4-(bis(4-fluorophenyl)(hydroxy)methyl)-2*H*-1,2,3-triazol-2-yl)methanone (33). The title compound was synthesized (*2R,5S*)-2-benzyl-5-((tert-butyldiphenylsilyl)oxy)piperidine (100 mg, 0.233 mmol), bis(4-fluorophenyl)(1*H*-1,2,3-triazol-4-yl)methanol (73.5 mg, 0.256 mmol) and HF-pyridine (2.45 mL, 2.69 mmol) according to the procedures described for compound **30**. This furnished N2-carbamoyl triazole urea **33** (18.3 mg, 0.036 mmol, 16% yield). $[\alpha]_D^{20}$ = 48 (*c* = 0.5, $CHCl_3$). HRMS [ESI+] m/z: calculated for $C_{28}H_{26}F_2N_4O_3$ $[M+H]^+$ 505.2046, found: 505.2045. ^{1}H NMR (600 MHz, $CDCl_3$) δ 7.72 (s, 1H), 7.33 – 7.31 (m, 6H), 7.03 – 6.99 (m, 7H), 4.65 (br s, 1H), 4.30 (br s, 1H), 3.54 (br s, 3H), 3.02 (br s, 2H), 1.57 – 1.32 (m, 5H). ^{13}C NMR (151 MHz, $CDCl_3$) δ 162.41 (d, *J* = 247.6 Hz), 152.82, 148.40, 140.91, 137.26, 133.37, 130.98, 129.13, 126.88, 124.21, 115. 22 (d, *J* = 21.1 Hz), 76.02, 51.09, 45.71, 41.81, 38.56, 37.57, 30.18, 27.42.

((*2R,5R)*-2-Benzyl-5-methoxypiperidin-1-yl)(4-(bis(4-fluorophenyl)(hydroxy)methyl)-2*H*-1,2,3-triazol-2-yl)methanone (34). The title compound was synthesized *(2R,5R)*-2-benzyl-

5-methoxypiperidine (100 mg, 0.487 mmol), bis(4-fluorophenyl)(1*H*-1,2,3-triazol-4-yl)methanol (154 mg, 0.536 mmol) according to the procedures described for compound **3**. The N2-carbamoyl triazole urea was isolated by silica gel chromatography (pentane/EtOAc 100:1 → 5:1) to afford 2,4-triazole urea **34** (70.7 mg, 0.136 mmol, 28% yield). $[\alpha]_D^{22}$ = -3.1 (*c* = 0.5, $CHCl_3$). HRMS [ESI+] m/z: calculated for $C_{29}H_{28}F_2N_4O_3$ $[M+H]^+$ 519.2202, found: 519.2203. ^{1}H NMR (400 MHz, $CDCl_3$) δ 7.53 (s, 1H), 7.32 – 7.19 (m, 9H), 7.04 – 6.92 (m, 4H), 4.84 – 3.93(m, 2H), 3.57 (br s, 1H), 3.50 – 3.33 (m, 3H), 3.25 (br s, 1H), 3.07 (br s, 1H), 3.03 – 2.92 (m, 2H), 2.05 (br s, 1H), 1.67 (br s, 3H). ^{13}C NMR (101 MHz, $CDCl_3$) δ 162.45 (d, *J* = 246.4 Hz), 155.75, 149.25, 140.68, 137.63, 135.27, 130.84, 129.05 (d, *J* = 8.1 Hz), 128.82, 126.93, 115.31 (d, *J* = 21.2 Hz), 76.58, 75.46, 56.35, 56.07, 46.52, 35.82, 25.59, 25.42.

(*(2R,5R)*-2-Benzyl-5-(cyclopropylmethoxy)piperidin-1-yl)(4-(bis(4-fluorophenyl)(hydroxy)methyl)-2*H*-1,2,3-triazol-2-yl)methanone (35). The title compound was synthesized from *(2R,5R)*-2-benzyl-5-(cyclopropylmethoxy)piperidine (50.0 mg, 0.204 mmol) according to the procedures described for compound **3**. The N2-carbamoyl triazole urea was isolated by silica gel chromatography (pentane/EtOAc 100:1 → 5:1) to afford 2,4-triazole urea (*(2R,5R)*-2-benzyl-5-(cyclopropylmethoxy)piperidin-1-yl)(4-(bis(4-fluorophenyl)(hydroxy)methyl)-2*H*-1,2,3-triazol-2-yl)methanone **35** (25.0 mg, 0.045 mmol, 22% yield). $[\alpha]_D^{20}$ = 21.4 (*c* = 0.5, $CHCl_3$). HRMS calculated for $C_{32}H_{33}F_2N_4O_3$ $[M+H]^+$ 559.2515, found: 559.2516. ^{1}H NMR (400 MHz, $CDCl_3$) δ 7.52 (br s, 1H), 7.32 – 7.27 (m, 6H), 7.17 (br s, 2H), 7.05 – 6.99 (m, 4H), 6.90 (br s, 1H), 4.65 (br s, 1H), 4.38 – 4.02 (m, 1H), 3.50 – 3.42 (m, 3H), 3.19 – 2.90 (m, 3H), 2.02 (br s, 1H), 1.80 – 1.62 (m, 3H), 1.12 – 0.90 (m, 1H), 0.57 (br s, 2H), 0.28 – 0.08 (m, 2H). ^{13}C NMR (101 MHz, $CDCl_3$) δ 162.48 (d, *J* = 251.5 Hz), 155.54, 149.15, 140.73, 137.68, 135.15, 130.92, 129.43, 129.09 (d, *J* = 8.1 Hz), 128.82, 126.91, 115.30

(d, *J* = 21.2 Hz), 76.60, 73.80, 56.49, 46.94, 44.55, 35.63, 26.10, 24.65, 11.05, 3.24.

((*2R,5S)*-2-Benzyl-5-methoxypiperidin-1-yl)(4-(bis(4-fluorophenyl)(hydroxy)methyl)-2*H*-1,2,3-triazol-2-yl)methanone (36). The title compound was synthesized from *(2R,5S)*-2-benzyl-5-methoxypiperidine (20.0 mg, 0.097 mmol) according to the procedures described for compound **3**. The N2-carbamoyl triazole urea was isolated by silica gel chromatography (pentane/EtOAc 100:1 → 5:1) to afford 2,4-triazole urea (*(2R,5S)*-2-benzyl-5-methoxypiperidin-1-yl)(4-(bis(4-fluorophenyl)(hydroxy)methyl)-2*H*-1,2,3-triazol-2-yl)methanone **36** (13.1 mg, 0.025 mmol, 26% yield). $[\alpha]_D^{22}$ = -8.1 (*c* = 0.4, $CHCl_3$). HRMS [ESI+] m/z: calculated for $C_{29}H_{28}F_2N_4O_3$ $[M+H]^+$ 519.2202, found: 519.2202. ^{1}H NMR (400 MHz, $CDCl_3$) δ 7.48 (s, 1H), 7.33 – 7.19 (m, 8H), 7.05 – 6.94 (m, 5H), 4.87 – 4.28 (m, 2H), 3.65 – 2.87 (m, 6H), 2.72 (br s, 4H), 2.09 – 1.83 (m, 2H), 1.54 – 1.39 (m, 1H). ^{13}C NMR (101 MHz, $CDCl_3$) δ 162.44 (d, *J* = 251.5 Hz), 155.37, 149.24, 140.83, 137.80, 134.91, 130.01, 129.18 (d, *J* = 9.1 Hz), 128.79, 126.89, 115.18 (d, *J* = 21.2 Hz), 76.57, 73.10, 56.63, 56.46, 45.70, 35.95, 23.09, 21.09.

((*2R,5S)*-2-Benzyl-5-(cyclopropylmethoxy)piperidin-1-yl)(4-(bis(4-fluorophenyl)(hydroxy)methyl)-2*H*-1,2,3-triazol-2-yl)methanone (37). The title compound was synthesized from *(2R,5S)*-2-benzyl-5-(cyclopropylmethoxy)piperidine (50.0 mg, 0.204 mmol) according to the procedures described for compound **3**. The N2-carbamoyl triazole urea was isolated by silica gel chromatography (pentane/EtOAc 100:1 → 5:1) to afford 2,4-triazole urea (*(2R,5S)*-2-benzyl-5-(cyclopropylmethoxy)piperidin-1-yl)(4-(bis(4-fluorophenyl)(hydroxy)methyl)-2*H*-1,2,3-triazol-2-yl)methanone **37** (23.9 mg, 0.043 mmol, 21% yield). $[\alpha]_D^{22}$ = -16 (*c* = 0.3, $CHCl_3$). HRMS calculated for $C_{32}H_{33}F_2N_4O_3$ $[M+H]^+$ 559.2515, found: 559.2516. ^{1}H NMR (400 MHz, $CDCl_3$) δ 7.47 (s, 1H), 7.34 – 7.24 (m, 5H), 7.19 (s, 3H), 7.04 – 6.99 (m, 5H), 4.56 (br s, 2H), 3.65 (br s, 1H), 3.31 (br d, *J* = 18.0 Hz, 1H), 3.11 (dd, *J* =

13.4, 6.9 Hz, 2H), 2.99 – 2.88 (m, 1H), 2.80 (br s, 2H), 2.24 – 2.03 (m, 1H), 1.96 – 1.77 (m, 2H), 1.47 –137 (m, 1H), 0.88 – 0.83 (m, 1H), 0.44 (br s, 2H), 0.12 (br s, 2H). ^{13}C NMR (101 MHz, $CDCl_3$) δ 162.46 (d, *J* = 248.5 Hz), 155.27, 150.05, 140.72, 137.85, 134.83, 129.22, 129.18 (d, *J* = 8.1 Hz), 129.04, 128.77, 126.85, 115.29 (d, *J* = 21.2 Hz), 76.57, 72.97, 55.84, 45.20, 42.84, 36.01, 24.09, 21.31, 10.73, 3.23.

ACKNOWLEDGEMENTS

This work was supported by the National Institutes of Health Grants DA033760 (to B.F.C.); grants from the Chinese Scholarship Council (to H.D.); the Netherlands Research Council–Chemical Sciences ECHO grant (to M.v.d.S.); and an ECHO-STIP Grant (M.v.d.S.). The authors declare no competing financial interest.

SUPPORTING INFORMATION

Supplemental Information includes additional biological figures, detailed experimental procedures for the synthesis of compounds **1-2** and the key intermediates, copies of NMR spectra of new compounds, and molecular formula strings. This material is available free of charge via the Internet at http://pubs.acs.org.

AUTHOR INFORMATION

Corresponding Author

* Phone: +31 71 527 4768. E-mail: m.van.der.stelt@chem.leidenuniv.nl.

ABBREVIATIONS

DAGL: diacylglycerol Lipase; DAG: diacylglycerol; ABHD6/11: α,β-hydrolase domain 6/11; APEH: acylaminoacyl-peptide hydrolase; PAFAH2: platelet activating factor acetylhydrolase 2; DDHD2: DDHD domain-containing protein 2; 2-AG: 2-arachidonoylglycerol; CB_1: cannabinoid receptor 1; LPS: lipopolysaccharide .

REFERENCES

(1) Adibekian, A.; Hsu, K. L.; Speers, A. E.; Brown, S. J.; Spicer, T.; Fernandez-Vega, V.; Ferguson, J.; Cravatt, B. F.; Hodder, P.; Rosen, H. Optimization and characterization of a triazole urea inhibitor for alpha/beta hydrolase domain-containing protein 11 (ABHD11): anti-probe for LYPLA1/LYPLA2 dual inhibitor ML211. In *Probe Reports from the NIH Molecular Libraries Program*, Bethesda (MD), March 31, 2010 - 2011, updated March 07, 2013.

(2) Adibekian, A.; Martin, B. R.; Wang, C.; Hsu, K. L.; Bachovchin, D. A.; Niessen, S.; Hoover, H.; Cravatt, B. F. Click-generated triazole ureas as ultrapotent in vivo-active serine hydrolase inhibitors. *Nat. Chem. Biol.* **2011,** *7*, 469-478.

(3) Hsu, K. L.; Tsuboi, K.; Chang, J. W.; Whitby, L. R.; Speers, A. E.; Pugh, H.; Cravatt, B. F. Discovery and optimization of piperidyl-1,2,3-triazole ureas as potent, selective, and in vivo-

active inhibitors of alpha/beta-hydrolase domain containing 6 (ABHD6). *J. Med. Chem.* **2013,** *56*, 8270-8279.

(4) Hsu, K. L.; Tsuboi, K.; Adibekian, A.; Pugh, H.; Masuda, K.; Cravatt, B. F. DAGLbeta inhibition perturbs a lipid network involved in macrophage inflammatory responses. *Nat. Chem. Biol.* **2012,** *8*, 999-1007.

(5) Inloes, J. M.; Hsu, K. L.; Dix, M. M.; Viader, A.; Masuda, K.; Takei, T.; Wood, M. R.; Cravatt, B. F. The hereditary spastic paraplegia-related enzyme DDHD2 is a principal brain triglyceride lipase. *Proc. Natl. Acad. Sci. U. S. A.* **2014,** *111*, 14924-14929.

(6) Bisogno, T.; Howell, F.; Williams, G.; Minassi, A.; Cascio, M. G.; Ligresti, A.; Matias, I.; Schiano-Moriello, A.; Paul, P.; Williams, E. J.; Gangadharan, U.; Hobbs, C.; Di Marzo, V.; Doherty, P. Cloning of the first sn1-DAG lipases points to the spatial and temporal regulation of endocannabinoid signaling in the brain. *J. Cell. Biol.* **2003,** *163*, 463-468.

(7) Reisenberg, M.; Singh, P. K.; Williams, G.; Doherty, P. The diacylglycerol lipases: structure, regulation and roles in and beyond endocannabinoid signalling. *Philos. Trans. R. Soc. Lond. B. Biol. Sci.* **2012,** *367*, 3264-3275.

(8) Tanimura, A.; Yamazaki, M.; Hashimotodani, Y.; Uchigashima, M.; Kawata, S.; Abe, M.; Kita, Y.; Hashimoto, K.; Shimizu, T.; Watanabe, M.; Sakimura, K.; Kano, M. The endocannabinoid 2-arachidonoylglycerol produced by diacylglycerol lipase alpha mediates retrograde suppression of synaptic transmission. *Neuron* **2010,** *65*, 320-327.

(9) Gao, Y.; Vasilyev, D. V.; Goncalves, M. B.; Howell, F. V.; Hobbs, C.; Reisenberg, M.; Shen, R.; Zhang, M. Y.; Strassle, B. W.; Lu, P.; Mark, L.; Piesla, M. J.; Deng, K.; Kouranova, E. V.; Ring, R. H.; Whiteside, G. T.; Bates, B.; Walsh, F. S.; Williams, G.; Pangalos, M. N.;

Samad, T. A.; Doherty, P. Loss of retrograde endocannabinoid signaling and reduced adult neurogenesis in diacylglycerol lipase knock-out mice. *J. Neurosci.* **2010,** *30*, 2017-2024.

(10) Baggelaar, M. P.; Janssen, F. J.; van Esbroeck, A. C.; den Dulk, H.; Allara, M.; Hoogendoorn, S.; McGuire, R.; Florea, B. I.; Meeuwenoord, N.; van den Elst, H.; van der Marel, G. A.; Brouwer, J.; Di Marzo, V.; Overkleeft, H. S.; van der Stelt, M. Development of an activity-based probe and in silico design reveal highly selective inhibitors for diacylglycerol lipase-alpha in brain. *Angew. Chem. Int. Ed. Engl.* **2013,** *52*, 12081-12085.

(11) Janssen, F. J.; Deng, H.; Baggelaar, M. P.; Allara, M.; van der Wel, T.; den Dulk, H.; Ligresti, A.; van Esbroeck, A. C.; McGuire, R.; Di Marzo, V.; Overkleeft, H. S.; van der Stelt, M. Discovery of glycine sulfonamides as dual inhibitors of sn-1-diacylglycerol lipase alpha and alpha/beta-hydrolase domain 6. *J. Med. Chem.* **2014,** *57*, 6610-6622.

(12) Bisogno, T.; Cascio, M. G.; Saha, B.; Mahadevan, A.; Urbani, P.; Minassi, A.; Appendino, G.; Saturnino, C.; Martin, B.; Razdan, R.; Di Marzo, V. Development of the first potent and specific inhibitors of endocannabinoid biosynthesis. *Biochim. Biophys. Acta, Mol. Cell Biol. Lipids* **2006,** *1761*, 205-212.

(13) Bisogno, T.; Burston, J. J.; Rai, R.; Allara, M.; Saha, B.; Mahadevan, A.; Razdan, R. K.; Wiley, J. L.; Di Marzo, V. Synthesis and pharmacological activity of a potent inhibitor of the biosynthesis of the endocannabinoid 2-arachidonoylglycerol. *Chem.Med.Chem.* **2009,** *4*, 946-950.

(14) Bisogno, T.; Mahadevan, A.; Coccurello, R.; Chang, J. W.; Allara, M.; Chen, Y. G.; Giacovazzo, G.; Lichtman, A.; Cravatt, B.; Moles, A.; Di Marzo, V. A novel fluorophosphonate inhibitor of the biosynthesis of the endocannabinoid 2-

arachidonoylglycerol with potential anti-obesity effects. *Br. J. of Pharmacol.* **2013,** *169*, 784-793.

(15) Ogasawara, D.; Deng, H.; Viader, A.; Baggelaar, M. P.; Breman, A.; den Dulk, H.; van den Nieuwendijk, A. M.; Soethoudt, M.; van der Wel, T.; Zhou, J.; Overkleeft, H. S.; Sanchez-Alavez, M.; Mo, S.; Nguyen, W.; Conti, B.; Liu, X.; Chen, Y.; Liu, Q. S.; Cravatt, B. F.; van der Stelt, M. Rapid and profound rewiring of brain lipid signaling networks by acute diacylglycerol lipase inhibition. *Proc. Natl. Acad. Sci. U. S. A.* **2016,** *113*, 26-33.

(16) Hsu, K. L.; Tsuboi, K.; Whitby, L. R.; Speers, A. E.; Pugh, H.; Inloes, J.; Cravatt, B. F. Development and optimization of piperidyl-1,2,3-triazole ureas as selective chemical probes of endocannabinoid biosynthesis. *J. Med. Chem.* **2013,** *56*, 8257-8269.

(17) Velmourougane, G.; Harbut, M. B.; Dalal, S.; McGowan, S.; Oellig, C. A.; Meinhardt, N.; Whisstock, J. C.; Klemba, M.; Greenbaum, D. C. Synthesis of new (-)-bestatin-based inhibitor libraries reveals a novel binding mode in the S1 pocket of the essential malaria M1 metalloaminopeptidase. *J. Med. Chem.* **2011,** *54*, 1655-1666.

(18) van den Nieuwendijk, A. M.; Ruben, M.; Engelsma, S. E.; Risseeuw, M. D.; van den Berg, R. J.; Boot, R. G.; Aerts, J. M.; Brussee, J.; van der Marel, G. A.; Overkleeft, H. S. Synthesis of L-altro-1-deoxynojirimycin, D-allo-1-deoxynojirimycin, and D-galacto-1-deoxynojirimycin from a single chiral cyanohydrin. *Org. Lett.* **2010,** *12*, 3957-3959.

(19) van der Wel, T.; Janssen, F. J.; Baggelaar, M. P.; Deng, H.; den Dulk, H.; Overkleeft, H. S.; van der Stelt, M. A natural substrate-based fluorescence assay for inhibitor screening on diacylglycerol lipase alpha. *J. Lipid Res.* **2015,** *56*, 927-935.

(20) Navia-Paldanius, D.; Savinainen, J. R.; Laitinen, J. T. Biochemical and pharmacological characterization of human alpha/beta-hydrolase domain containing 6 (ABHD6) and 12 (ABHD12). *J. Lipid Res.* **2012,** *53*, 2413-2424.

(21) Manabe, K. Synthesis of novel chiral quaternary phosphonium salts with a multiple hydrogen-bonding site, and their application to asymmetric phase-transfer alkylation. *Tetrahedron* **1998,** *54*, 14465-14476.

(22) Di Marzo, V.; Matias, I. Endocannabinoid control of food intake and energy balance. *Nat. Neurosci.* **2005,** *8*, 585-589.

(23) Boon, M. R.; Kooijman, S.; van Dam, A. D.; Pelgrom, L. R.; Berbee, J. F.; Visseren, C. A.; van Aggele, R. C.; van den Hoek, A. M.; Sips, H. C.; Lombes, M.; Havekes, L. M.; Tamsma, J. T.; Guigas, B.; Meijer, O. C.; Jukema, J. W.; Rensen, P. C. Peripheral cannabinoid 1 receptor blockade activates brown adipose tissue and diminishes dyslipidemia and obesity. *FASEB J.* **2014,** *28*, 5361-5375.

(24) Powell, D. R.; Gay, J. P.; Wilganowski, N.; Doree, D.; Savelieva, K. V.; Lanthorn, T. H.; Read, R.; Vogel, P.; Hansen, G. M.; Brommage, R.; Ding, Z. M.; Desai, U.; Zambrowicz, B. Diacylglycerol lipase alpha knockout mice demonstrate metabolic and behavioral phenotypes similar to those of cannabinoid receptor 1 knockout mice. *Front. Endocrinol. (Lausanne)* **2015,** *6*, 86.

(25) Di Marzo, V.; Goparaju, S. K.; Wang, L.; Liu, J.; Batkai, S.; Jarai, Z.; Fezza, F.; Miura, G. I.; Palmiter, R. D.; Sugiura, T.; Kunos, G. Leptin-regulated endocannabinoids are involved in maintaining food intake. *Nature* **2001,** *410*, 822-825.

Table of Contents graphic